STEADY STATE & TRANSIENT ANALYSIS OF CONVERTER CONTROLLED DC SERIES MOTOR

A Thesis Submitted
in Partial Fulfilment of the Requirements
for the Degree of

MASTER OF TECHNOLOGY

By

BHUDEO SHARMA

to the

DEPARTMENT OF ELECTRICAL ENGINEERING

INDIAN INSTITUTE OF TECHNOLOGY KANPUR

JULY, 1981

** परम पूज्य पिताजी के चरणों में **

EE-1981-M-SHA-STE

CERTIFICATE

Certified that this work 'Steady-state and Transient Analysis of Converter-controlled D.C. Series Motor' by Shri Bhudeo Sharma has been carried out under my supervision and has not been submitted elsewhere for a degree.

(G.K. Dubey)
Professor
Department of Electrical Engineering
Indian Institute of Technology
Kanpur-208016

ACKNOWLEDGEMENT

I wish to express my deep sense of gratitude to Dr. G.K. Dubey for suggesting me this topic and also for his able and dynamic guidance in the course of this project.

I wish to thank my freinds - Mr. P. Subbanna Bhat, Mr. Rana Ghosh, Mr. Pankaj D. Parikh, Mr. Prem Chand Pandey, Mr. H.S. Satpathi, Mr. H.K. Patel and Mr. A.J. Kellogg for their help at various stages of this work.

Thanks are also due to all the staff members of all the laboratories whose help I had received directly or indirectly in carrying out this work.

I am also thankful to Mr. J.S. Rawat for his excellent typing.

Last but not the least, I am thankful to Mr. E.S.N. Prasad for his help in proof reading.

Bhudeo Sharma

TABLE OF CONTENTS

ABSTRACT

The steady-state and transient analysis methods of d.c. series motor reported so far do not take into account the non-linearity of the magnetic circuit. Furthermore, for transient analysis discontinuous conduction has been neglected and only first-order model has been reported though a series motor is essentially a second-order system. This thesis deals with the steady-state and transient analysis methods for fully-controlled and half-controlled converter fed d.c. series motor taking non-linearity and discontinuous condution into account. For transient analysis first-order as well as second-order models have been considered. A method has also been described for selecting a suitable value of filter inductance which eliminates discontinuous conduction and keeps the ripple within permissible values. Theoretical deductions have been verified experimentally. A single phase firing circuit suitable for fully-controlled converter, fully-controlled converter with half-controlled characteristics, sequence control, symmetrical pulse-width modulation with one pulse per half cycle and asymmetrical control has been fabricated.

LIST OF SYMBOLS

i	instantaneous value of armature current, amps.
E	induced armature voltage, volts
Em	Maximum value of ac supply voltage, volts
w	frequency of ac supply, rad/sec
i_{av}	average value of armature current, amps
i_{avo}	steady state value of i_{av}, amps.
Δi_{av}	small increment in i_{av}, amps
W	instantaneous value of motor speed, rad/sec
W_{av}	average value of motor speed, rad/sec
W_{avo}	average speed during steady-state operation, rad/sec
ΔW_{wav}	small increment in W_{av}, rad/sec
R	total armature circuit resistance, ohms.
L	total armature circuit inductance, henry
T_a	armature time constant, L/R, sec
T_{m1}	mechanical time constant, J/B, sec
T_{m2}	time constant $JR/(BR+K^2)$, sec
B	viscous friction coefficient, Nm/rad/sec
J	polar moment of inertia of motor and load, $Kg\text{-}m^2$.
K	motor induced emf constant, volts/rad/sec.
K_o	value of K at steady-state operating point, volts/rad/sec.
M_{af}	constant K/i_{av}, volts sec/amp. rad
M_{afo}	value of M_{af} for steady state operation, volts sec/amp. rad

T_L	Load torque, Nm
ΔT_L	small increment in T_L, Nm
α	firing angle of thyristor in the converter, rad
W_c	critical value of speed, rad/sec
T_c	value of torque corresponding to W_c, Nm
s	laplace variable
t	time, sec
$i_{d1}(n)$	initial value of current in duty interval of nth cycle, amps.
$W_{d1}(n)$	initial value of speed in duty interval of nth cycle, rad/sec.
β	angle at which armature current becomes zero.
i_d, i_f	instantaneous armature currents during duty, freewheeling intervals, amps.
W_p	normalized value of speed
T_p	normalised value of torque
p	differential operator
K_{re}	emf due to residual magnetism, V/(rad/sec)
i_α	instantaneous armature current at triggering angle α.
i_{FW}	instantaneous armature current 180° or 0°
S_1	percentage deviation of average current from rms current.
V'_{av}	rate of change of applied voltage with firing angle
I	rms value of current, A

FIGURE CAPTIONS

Fig. No.	Caption
1	DC series motor fed by (a) fully-controlled and (b) half-controlled converters
2.1,2.2	Closed-loop block diagrams of series motor for small perturbations.
2.3	Various approximations of magnetisation characteristic
3.1	Various modes of operation
3.2	Steady-state speed-torque characteristic of motor fed by fully-controlled converter _____ Computed x x x x Experimental
3.3	Steady-state speed torque characteristic of motor fed by half-controlled converter. _____ Computed x x x x Experimental
3.4	Variation of CRF with p.u. input voltage for both fully-controlled (FC) and half-controlled (HC) converter fed d.c. series motor _____ Computed x x x x Experimental
3.5	Boundaries between continuous and discontinuous conduction on normalized speed-torque plane - - - - minimum speed-torque curve
4.1	Closed loop block digram of series motor for small perturbation using first-order model.

Fig. No.	Caption
4.2	Closed loop block diagram of series motor for small perturbation using second-order model.
4.3	Starting transients of half-controlled converter fed dc series motor for (a) $\alpha = 120°$, generator load = 3.83 W_{av} (b) $\alpha = 105°$, generator load = 6.26 W_{av} _____ step-by-step method - - - method II -.-.- method I x x x experimental
4.4	Transient response of half-controlled converter fed d.c. series motor for an input perturbation, using method II. (a) $\alpha_0 = 120°$, $W_{avo} = 0.405$ p.u. T changes from 3.83 W_{av} to 0.65 W_{av}. (b) $\alpha_0 = 120°$, $W_{avo} = 0.405$ p.u. $i_{avo} = 0.4$ p.u., $\Delta\alpha = 4°$
4.5	Transient response for fully-controlled converter fed d.c. series motor $\alpha = 72°$, generator load = 1.5 W_{av} oooo step-by-step method -.-.- method I - - - method II x x x experimental
4.6	Transient response of d.c. series motor fed by half-controlled converter (a) $\alpha = 120°$, $T_L = 0.59$ p.u. (b) $\alpha_0 = 120°$, $W_{avo} = .185$ p.u. $i_{avo} = 0.65$ p.u. $\Delta T_L = .17$ p.u. (c) $\alpha_0 = 120°$, $W_{avo} = .185$ p.u., $i_{avo} = .65$ p.u $\Delta\alpha = 5°$ _____ step-by-step oooo method I • • • method II

Fig. No.	Caption
4.7	Effect of inductance on transient response $\alpha = 120°$, $T_L = .59$ p.u. ____ L = 0.076H ..... L = 0.176H
4.8	Magnetisation characteristic of the motor.
5.1	Firing scheme
5.2	Firing circuit
5.3	Output waveforms at various stages

CHAPTER 1

INTRODUCTION

Solid state d.c. drives find wide use in applications requiring variable speed, good regulation, frequent starting and reversing, and are widely employed in rolling mills, paper mills, minewinder, machine tools etc. The single phase half-controlled and fully-controlled converter fed d.c. series motor is mainly employed in main-line-traction and crane applications. The present thesis deals with certain aspects of converter controlled d.c.drive incorporating d.c. series motor.

The main problem in the analysis of the converter-fed d.c. series motor for steady-state and transient conditions arises due to the non-linear relation between the armature induced voltage and the armature current. Because of this the differential equations that describe the operation of the motor in the different modes of the converter cycle are nonlinear. Accurate solution of these equations for steady-state and transient conditions, can only be obtained numerically by the use of considerable computation time. The reported methods for determining the performance of the motor under steady-state and transient conditions do not take above

nonlinear relationship into account . These methods reported so far have been reviewed in Chapter 2.

1.1 Steady-state analysis & selection of filter inductance:

A steady-state analysis method for half-controlled converter fed d.c. series motor has been described by Doradla and Sen [1] based on mode-by-mode solution of differential equations using final condition of the previous mode as initial condition for each successive mode. It uses a linear model of d.c. series motor and, therefore, gives inaccurate results. The authors have not given any experimental verification of predicted results for speed-torque characteristics. Also, as it involves mode-by-mode solution of differential equations, the computation effort and time is large.

A method for determining the performance of the d.c. series motor fed by half-controlled and fully-controlled converters has been developed and presented in Chapter 3 of the thesis. The method takes into account nonlinearity of the magnetic circuit. While the discontinuous conduction for fully-controlled converter case has been taken into account, an elegant method for calculation of optimum value of filter inductance so as to eliminate discontinuous conduction and keep the a.c. ripple within acceptable limits, has

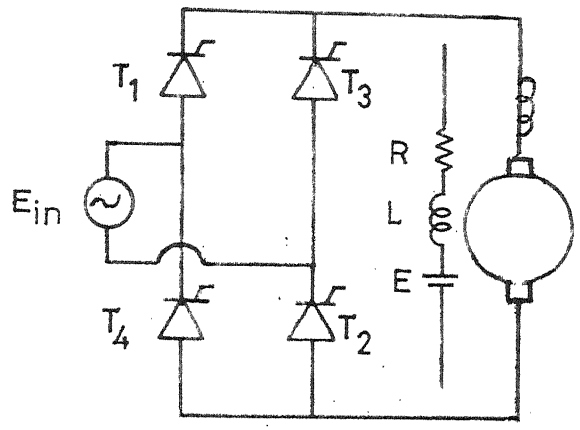

(a)

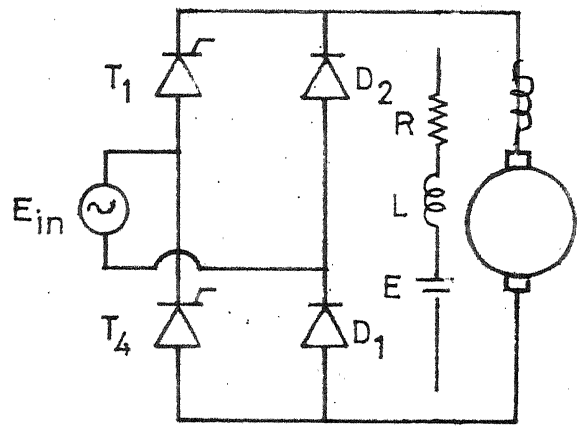

(b)

Fig.1. DC series motor fed by

(a) fully-controlled converter
(b) half-controlled converter

been presented. Monograms have been given in terms of normalised variables so as to be used by any series motor controlled by fully-controlled converter. The results have been verified experimentally.

1.2 Transient Analysis:

A transient analysis method for half-controlled converter fed d.c. series motor has been presented by Ramamoorthy and Ilango [2]. It essentially consists of obtaining an approximate first-order continuous model for small perturbations of firing angle and load torque. As it uses only linear model, it is inaccurate and particularly not suitable for calculating transients with large parturbations and starting process. Armature circuit time constant has been neglected, thus giving a first-order approximation of a system which is actually of second-order. Therefore, considerable error is introduced for medium and large size motors, where armature circuit time constant cannot be neglected. The error is particularly large in current-time curve as the nature of the predicted curve itself is different from the actual one. Also it cannot be adopted for fully-controlled converter, where discontinuous conduction must be taken into account. In the present work methods of transient analysis of series motor fed by half-controlled and

fully-controlled converters have been developed and have been reported in Chapter 4. Both the first-order and second-order models have been developed. The nonlinearity of the magnetic circuit and discontinuous conduction have been taken into account. These methods involve considerably less computation time compared with that involved in point-by-point method and also take care of the small and large perturbations. The computed results have been compared with those obtained experimentally.

1.3 Converter firing control circuit:

In chapter 5 of the thesis, a firing control circuit is given. This circuit is simple and suitable for various converter operations such as i) fully-controlled operation, ii) fully-controlled operation with half-controlled characteristics, iii) sequence control, iv) symmetrical pulse width modulation with one pulse per half cycle and v) asymmetrical triggering control. The same principle can be extended to 3-phase a.c. voltage controller and 3-phase thyristor bridge converter operation. The circuit is stable and immune to stray pulses and noise unlike monostable circuits.

CHAPTER 2

LITERATURE REVIEW

2.1 Introduction:

Solid state control plays an important role in the control of d.c. drive systems. Recently solid state d.c. drives are fast replacing the conventional Ward-Leonard Motor-Generator set. Such drives have numerous outstanding advantages, such as minimal maintenance, less space and weight, higher efficiency, faster time response and so on. Series motor which is particularly suitable for constant horse-power drive, has an important application in the traction system. Previously, the normal practice was to operate the d.c. traction motors from d.c. source with insignificant amount of ripple content, derived from multiphase rectifiers. At present, with the availablity of high power thyristor switches, series motor drives fed from 50 Hz supply are being economically employed, phase-control scheme being normally used to control speed of such d.c. drives.

Methods of determining the performance of the thyristor controlled series motor have been earlier reported by authors referred to in [1], [2] and [3]. In this chapter, these methods have been reviewed and their advantages and limitations discussed.

2.2 Modelling of Thyristor-controlled Series Motor:

Doradla and Sen [1] have presented a method for calculating the performance of d.c. series motor fed by a half-controlled converter which may be operated with phase-control or current-control.

The equations governing the operation of series motor fed by half-controlled converter under phase-control scheme are given as follows:

Mode 1: Thyristor conducts:

$$E_m \sin \omega t = Ri + L\,pi + M_{af}\, i\, W + K_{re} W \qquad \alpha \leq \omega t \leq \pi \tag{2.1}$$

$$M_{af}\, i^2 = J\, pW + BW + T_L \tag{2.2}$$

Mode 2: Free wheeling action takes place

$$0 = Ri + Lpi + M_{af}\, i\, W + K_{re} W \qquad \pi \leq \omega t \leq (\pi + \alpha) \tag{2.3}$$

or

$\pi \leq \omega t \leq (\pi + \beta)$ if Mode 3 is present.

$$M_{af} \cdot i^2 = J\, pW + BW + T_L \tag{2.4}$$

Mode 3: Armature current is zero and motor coasts

$$i = 0 \quad (\pi + \beta) \leq \omega t \leq (\pi + \alpha) \tag{2.5}$$

$$T_d = 0 = J\, pW + BW + T_L \tag{2.6}$$

The performance characteristics of the motor can now be obtained by solving equations (2.1)-(2.6) numerically. Since the computation is to be carried out from standstill to steady-state speed of the drive, it requires computation over many cycles before steady-state condition is reached. A time sharing method is given in which case a steady-state speed W_{av} is assumed and then only eqns. (2.1), (2.3) and (2.5) have to be considered. This also makes it possible to obtain an analytical expression for the armature current. Thus the solutions of equations (2.1) and (2.3) assuming constant speed are as given below:

Mode 1: Thyristor conducts

$$i = (Em/L\,(w^2+k_1^2)^{1/2})(\sin wt-\tan^{-1}(w/k_1)) - \sin(\alpha-\tan^{-1}(w/k_1))\exp((-k_1/w)(wt-\alpha))+ i_\alpha \exp((-k_1/w)(wt-\alpha)) + (K_{re}\,W_{av}/Lk_1).(\exp((-K_1/w)(wt-\alpha))-1)$$

$$\alpha \leq wt \leq \pi \qquad (2.7)$$

Mode 2: Free wheeling action takes place

$$i = i_{FW}\exp((-k_1/w)(wt-\pi))-(K_{re}\,W_{av}/L\,k_1).(1-\exp((-k_1/w)(wt-\pi)))$$

(2.8)

$\pi \leq wt \leq (\pi+\alpha)$ if mode 3 is absent

$\pi \leq wt \leq (\pi+\beta)$ if mode 3 is present

where $k_1 = (R+M_{af}\,W_{av})/L$

Mode 3: Motor armature current is zero.

$$i = 0 \quad (\pi + \beta) \leq \omega t \leq (\pi + \alpha) \qquad (2.9)$$

Now equations (2.7)-(2.9) can be used to compute the armature current during each cycle for a particular triggering angle, and steady-state condition is noted by noting the variation of average current over successive cycles. By this method, the steady-state is reached after only a few cycles of computation. The performance characteristics are determined after the steady-state condition is reached.

It is seen in the above analysis that the M_{af}, the mutual armature circuit inductance is constant, i.e., the magnetic circuit has been assumed linear. This will result in appreciable error. The time-saving method involves mode-by-mode solutions of differential equations, the computation time is still large.

Ramamoorthy and Ilango [2] have analysed the half-controlled converter fed series motor in its application as servomotor and suggested a method of obtaining its transient response by perturbation techniques. The motor being nonlinear, the analysis holds for small perturbations around a given steady-state operating point. The parameters for any

given operating point can be determined by taking into account all nonlinearities and treating these parameters as constants for small perturbations around that operating point. The block diagram and transfer functions are developed for any general operating point, and analytical expressions are derived for the transient response during small torque or firing angle changes.

The differential equations governing the performance of series motor are nonlinear; therefore, it is not possible to derive analytically a transfer function that will be valid under all conditions. However, transfer functions that will be valid for small perturbations may be derived under certain simplifying assumptions, the parameters being dependent on the given steady-state operating point. The differential equation governing the steady-state as well as transient operation of the series motor may be written as

$$Em \sin wt = Ri + pL\, i + W M_{af}\, i \qquad (2.10)$$

The armature ~~induc~~resistance R and mutual inductance M_{af} being dependent on the current, the equation is nonlinear. The prediction of transient behaviour is confined to the determination of the temporal variation of the average values rather than the instantaneous values of current and speed, for any given disturbances. In terms of average

values, equation (2.10) may be written as

$$E_{av}(\alpha) = RI_{av} + M_{af} W_{av} I_{av} \qquad (2.11)$$

where

$$E_{av}(\alpha) = \frac{Em}{\pi} (1 + \cos\alpha)$$

The differential equation controlling the dynamics of the series motor is

$$BW + pJ W = M_{af} i^2 - T_L \qquad (2.12)$$

Since prediction of transients in average current and average speed only is desired, the above equation which is valid at every instant, when M_{af} is chosen according to the instantaneous value of current, is rewritten as

$$BW_{av} + pJ W_{av} = M_{af} I^2 - T_L \qquad (2.13)$$

For (2.13) to be compatible with (2.11), Let

$$k = I/I_{av} \qquad (2.14)$$

$$S_1 = \left(\frac{I}{I_{av}} - 1\right) \times 100 \qquad (2.15)$$

The authors have obtained the variation of S_1 with load torque and firing angle numerically and it is shown that S_1 is very small and hence k is very close to unity over the entire operating range.

Thus, from equation (2.13)

$$BW_{av} + pJ\ W_{av} = M_{af}\ k^2\ I_{av}^2 - T_L \qquad (2.16)$$

where the value of k corresponds to the operating point.

To obtain the block diagram of the series motor using perturbation techniques, from equation (2.11)

$$V_{avo}'(\alpha).\Delta\alpha = M_{afo}\ I_{avo}\ \Delta W_{av} - Z_o\ \Delta i_{av} \qquad (2.17)$$

where

$$V_{avo}'(\alpha) = -\frac{Em}{\pi}\sin\alpha \quad \text{and} \quad Z_o = R_o + M_{afo}\ W_{avo}$$

Also from (2.16)

$$(B + pJ)\Delta W_{av} = 2\ M_{afo}\ k_o^2\ I_{avo}\ \Delta i_{av} - \Delta T_L \qquad (2.18)$$

From (2.17) and (2.18), a simple closed-loop block diagram for small perturbations with parameters depending on the operating point is drawn in Fig. 2.1. Now the transient response can be easily derived from the block diagram.

Let the firing angle be constant and load torque suddenly changed by ΔT_L.

Then

$$\Delta W_{av(s)} = -\frac{\Delta T_L(s)}{s}\ \frac{1}{(D_o + sJ)} \qquad (2.19)$$

$$\Delta W_{av}(t) = - \frac{\Delta T_L}{D_o} \left(1-e^{-t/T_o}\right) \qquad (2.20)$$

where,

$$D_o = B + \frac{2 M_{afo}^2 I_{avo}^2 k_o^2}{Z_o} \text{ and } T_o = \frac{J}{D_o}$$

and

$$\Delta i_{av}(s) = - \frac{M_{afo} I_{avo} \Delta W_{av}(s)}{Z_o} \qquad (2.21)$$

$$\Delta i_{av}(t) = \frac{M_{afo} I_{avo}}{D_o Z_o} \left(1-e^{-t/T_o}\right) \Delta T_L \qquad (2.22)$$

Now let the load torque remain constant and firing angle suddenly changed by $\Delta\alpha$. Then from the block diagram of Fig. 2.1.

$$\Delta W_{av}(s) = \frac{2M_{afo} k_o^2 I_{avo} V'_{avo}(\alpha)}{Z_o} \frac{\Delta\alpha(s)}{s(D_o+sJ)} \qquad (2.23)$$

and

$$\Delta i_{av}(s) = \frac{1}{Z_o} \left(V_{avo}'(\alpha) \Delta\alpha(s) - M_{afo} I_{avo} \Delta W_{av}(s)\right) \qquad (2.24)$$

To obtain the values of W_{avo}, I_{avo} and k_o in the above eqns. corresponding to any given operating point, the numerical method has to be resorted to before the transient response

around this operating point is found. However, once the performance curve of the series motor giving the steady-state values of W_{av}, I_{av} and S_1 for various firing angles and load torques are numerically obtained and plotted, the values can be easily read off for any given operating point.

It's, however, seen that the above method neglects armature circuit time constant and is a linear first-order approximation of a system which is actually of second order, particularly when the medium and large size motors are involved. Also it is not suitable for starting transients where nonlinearity has to be taken into account.

Bhadra[3] has given a method to predict the transient response of d.c. series motor driven by thyristor chopper or half-controlled rectifier, taking into consideration the electrical time constant of armature circuit. Again, small disturbance is assumed and nonlinear differential equations have been linearized around a given steady-state operating point. The basic differential equation describing the electrical behaviour of the motor is

$$Ri + pLi + M_{af} Wi = v \qquad (2.25)$$

where, $v = 0$ for $0 \leq t \leq T_{off}$

$v = v(t)$ for $T_{off} \leq t \leq T$

Each of the variable quantities in the above equation may be expressed as the sum of a steady-state component and a time-varying component as follows.

$$\begin{aligned} i &= I_{avo} + i_1 \\ v &= V_{avo} + v_1 \\ W &= W_{avo} + w_1 \end{aligned} \qquad (2.26)$$

For half-controlled converter with firing angle α

$$\begin{aligned} V_{avo} &= \frac{Em}{\pi} \ (1 + \cos\alpha) \\ v_1 &= -V_o \text{ for } 0 \leq wt \leq \alpha \\ v_1 &= Em \sin(wt) - V_o \text{ for } \alpha \leq wt \leq \pi \end{aligned} \qquad (2.27)$$

For chopper case,

$$\begin{aligned} V_{avo} &= \frac{T_{ON}}{T} E \\ v_1 &= -\frac{T_{ON}}{T} E \quad \text{for } 0 \leq t \leq T_{off} \\ v_1 &= E - \frac{T_{ON}}{T} E \text{ for } T_{off} \leq t \leq T \end{aligned} \qquad (2.28)$$

From equations (2.25) and (2.26), neglecting small quantities,

$$Lp\, i_1 + R(I_{avo} + i_1) + M_{af}(W_{avo}\, I_{avo} + w_1\, I_{avo} + W_{avo}\, i_1) = V_{avo} + v_1 \qquad (2.29)$$

separating the steady-state and time varying components,

$$R\, I_{avo} + M_{af}\, W_{avo}\, I_{avo} = V_{avo} \qquad (2.30)$$

$$L\, p i_1 + R\, i_1 + M_{af}(I_{avo}\, w_1 + W_{avo}\, i_1) = v_1 \qquad (2.31)$$

The average value of current i is defined as

$$I_{av} = \frac{1}{T} \int_0^T i\, dt = \frac{1}{T} \int_0^T (I_{avo} + i_1)\, dt = I_{avo} + \Delta i_{av} \qquad (2.32)$$

Similarly W_{av} and V_{av} can be difined. The value of k is assumed constant at k_o.

As the prediction of the transient behaviour is confined to the determination of the changing incremental average values of current and speed, i.e., Δi_{av} and ΔW_{av}, rather than their total instantaneous values consequent on small perturbations, equation (2.31) may be written as

$$Lp\, \Delta i_{av} + R\, \Delta i_{av} + M_{af}(I_{avo}\, \Delta W_{av} + W_{avo}\, \Delta i_{av}) = \Delta V_{av} \qquad (2.33)$$

From the dynamics of the motor,

$$J\, pW + T_L + BW = M_{af}\, i^2 \qquad (2.34)$$

For a given operating point of steady operation

$$T_L + BW_{avo} = M_{af}\, I_{avo}^2 \qquad (2.35)$$

Rewriting eqn. (2.34),

$$T_L + \Delta T_L + B(W_{avo} + \Delta W_{av}) + J\, p \Delta W_{av} = M_{af}\, k_o^2\, (I_{avo} + \Delta i_{av})^2 \qquad (2.36)$$

or $$J\, p\, \Delta W_{av} + \Delta T_L + B \Delta W_{av} = 2k_o^2\, M_{af}\, I_{avo} \Delta i_{av} \qquad (2.37)$$

Laplace transforming equations (2.33) and (2.37)

$$\Delta i_{av}(s) = \frac{\Delta V_{av}(s) - M_{af}\, I_{avo}\, \Delta W_{av}(s)}{R' + sL} \qquad (2.38)$$

$$\Delta W_{av}(s) = \frac{2k_o^2\, I_{avo}\, \Delta i_{av}(s) - \Delta T_L(s)}{B + sJ} \qquad (2.39)$$

where $R' = R + M_{af}\, W_{avo}$

The block diagram based on equations (2.38) and (2.39) is shown in Fig. 2.2. The response to changes in voltage and torque can now be found from the block diagram.

Though electrical time constant has been considered, this approach is not suitable for large transients such as starting process.

In all the methods described above, only half-controlled converter has been considered. No suitable methods of steady-state and transient analysis have been reported for

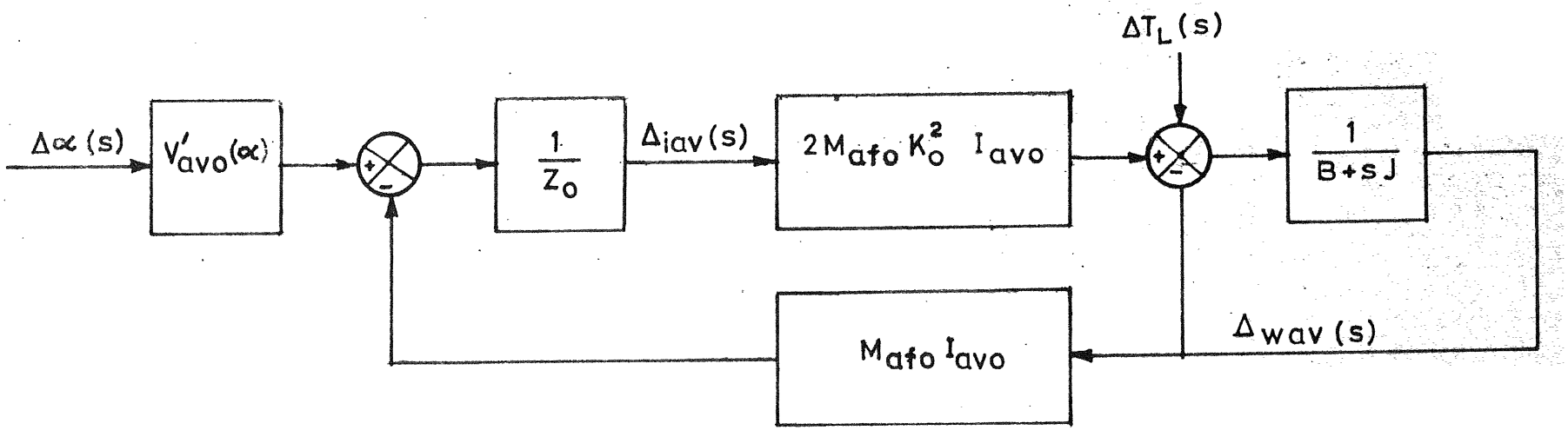

Fig. 2.1

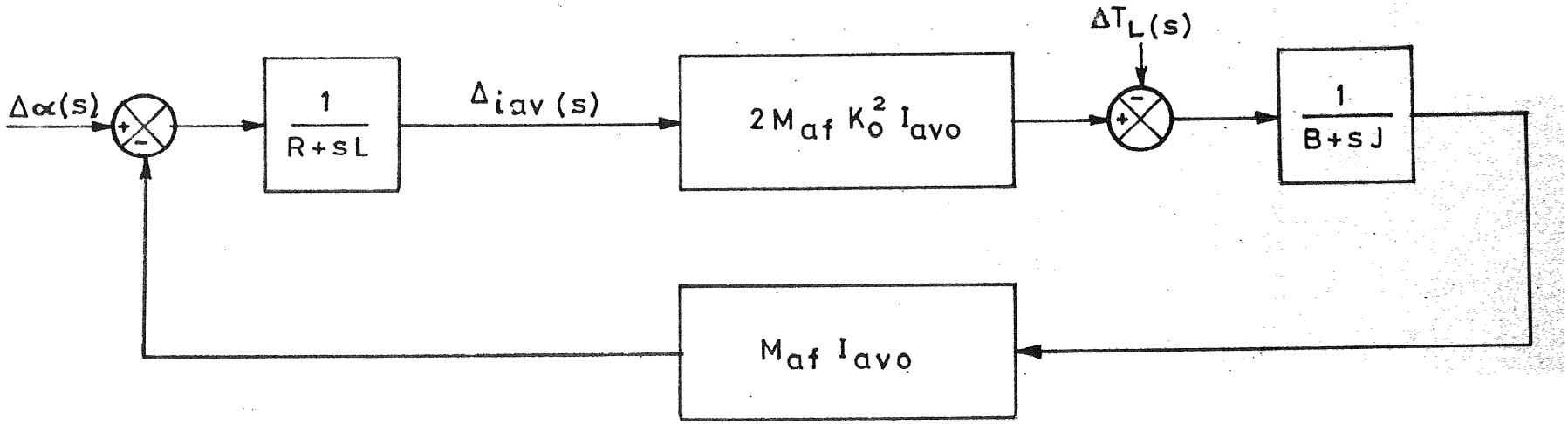

Fig. 2.2 Closed loop block diagrams of sereis motor for small purturbations

fully-controlled converter case taking discontinuous conduction and nonlinearity of the magnetic circuit into account. No attempt has also been made for predicting ripple in armature current when fed by half-controlled or fully-controlled converter.

2.3 Non-linearity of magnetic circuit &its approximation:

The difficulty in the analysis of series motor arises because of the nonlinearity of magnetic circuit, which makes the governing equations nonlinear. In the methods of analysis proposed in the following chapter, the motor constant K is assumed to be a function of the average value i_{av} of the armature current rather than that of instantaneous value. Thus

$$K = f(i_{av}) \qquad (2.40)$$

During a given converter cycle, i_{av} is fixed so that K is also fixed. The value of K for a given i_{av} is obtained from the magnetisation characteristic of the motor.

For any small increment Δi_{av} in the average value of the current, the magnetisation characteristic can be approximated by the three approaches shown in Fig.2.3, for two values of i_{av}, i.e., i_{o1} and i_{o2}.

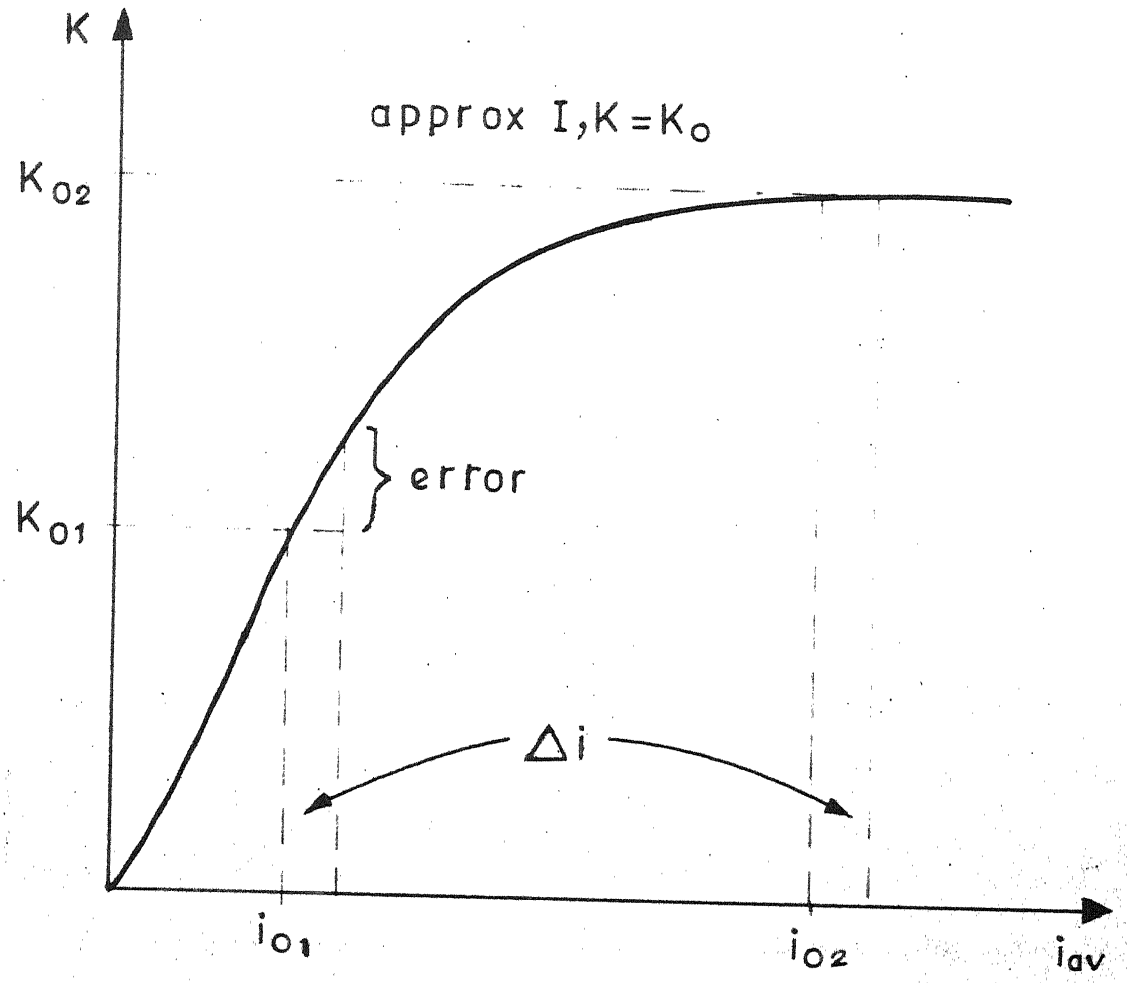

Fig. 2.3a Magnetisation characteristic approximation I

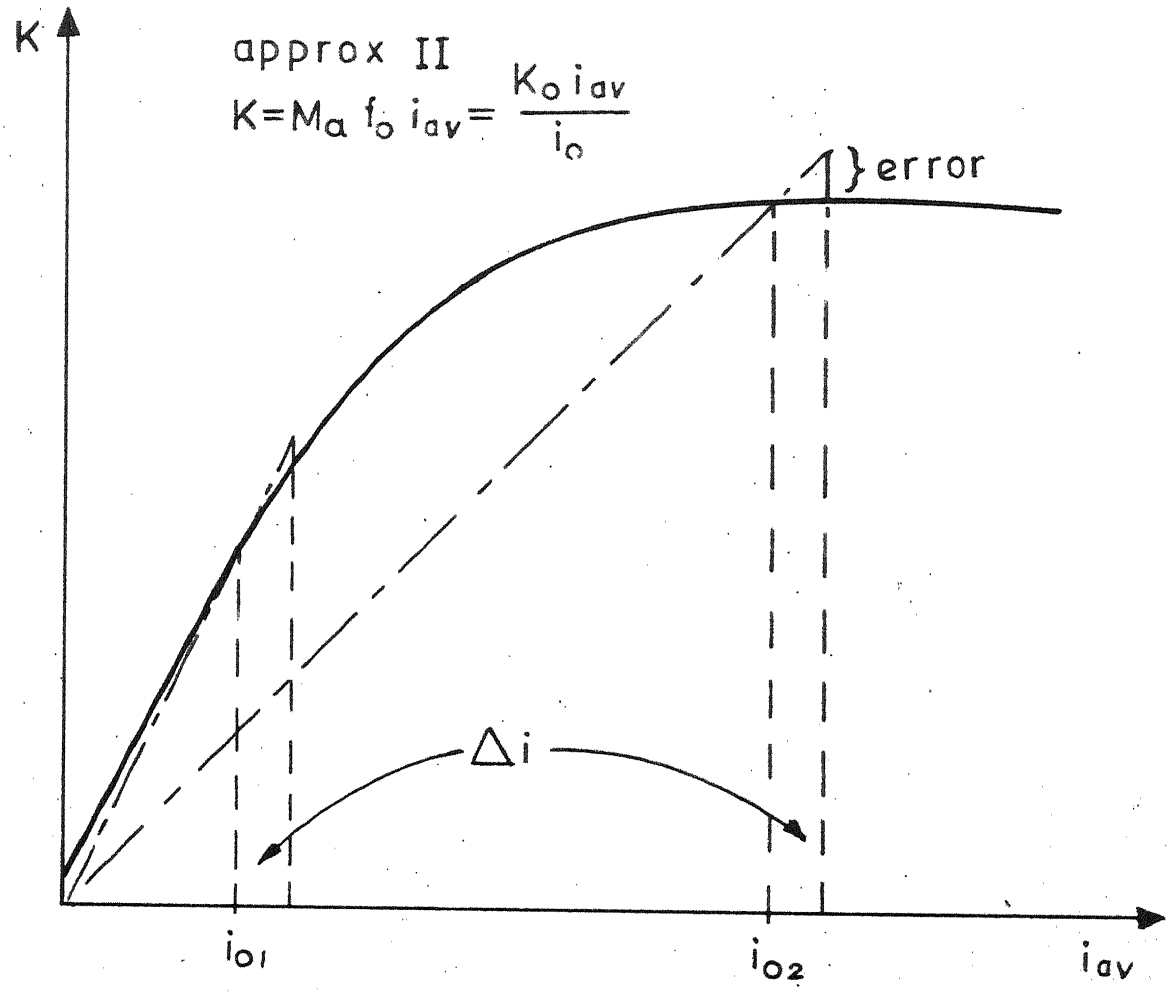

Fig. 2.3b Magnetisation characteristic approximation II

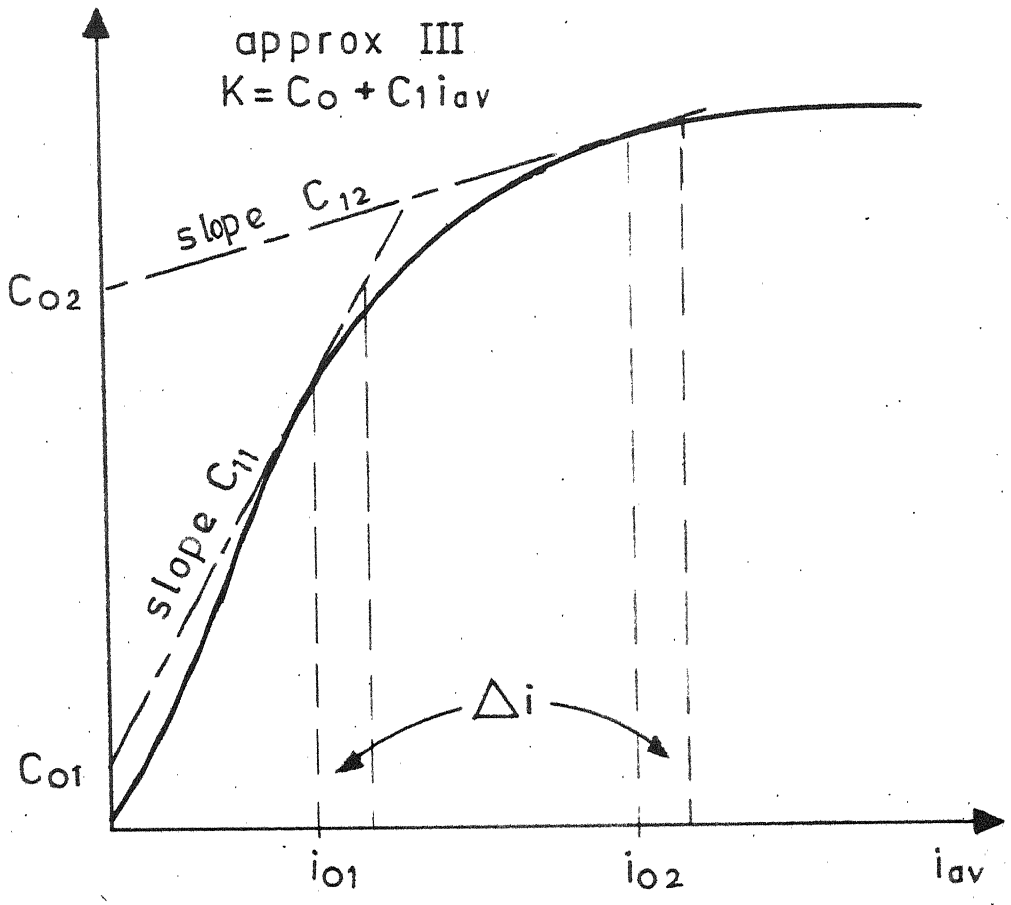

Fig. 2.3c Magnetisation characteristic approximation III

In Fig. 2.3(a), it is assumed that K_o remains constant for a small increment of current. Thus,

$$K = K_o \tag{2.41}$$

In Fig. 2.3(b), the magnetisation characteristic has been approximated by a straight line passing through the point corresponding to the value of current under consideration and the origin. Thus

$$K = M_{afo}\, i_{av} \tag{2.42}$$

where, $M_{afo} = \frac{K_o}{i_o}$

In Fig. 2.3(c) the magnetisation characteristic is approximated by a straight line passing through the point under consideration and has the same slope as that of magnetisation characteristic at that point, i.e.,

$$K = C_o + C_1\, i_{av} \tag{2.43}$$

The approximations of Fig. 2.3(a),(b) and (c) are termed as approximations I,II and III respectively.

CHAPTER 3

STEADY-STATE ANALYSIS OF CONVERTER CONTROLLED D.C. SERIES MOTOR

3.1 Introduction:

The following assumptions are made initially:

i) Thyristors and diodes are ideal switches.

ii) The motor field and armature resistances and inductances are constant.

In case of half-controlled converter feeding a d.c. series motor, if residual magnetism and the drops across thyristors and diodes are neglected, the possibility of discontinuous conduction taking place can be ignored. Even if the above considerations are taken into account, the discontinuous conduction occurs only in very narrow range of speed-torque characteristics. Hence, it can always be ignored. However, in case of fully-controlled converter fed d.c. series motor, the discontimuous conduction does take place for wide range of load torque because current has to flow against the supply voltage during regeneration interval. Hence, it must be taken into account in the analysis of series motor fed by fully-controlled converter.

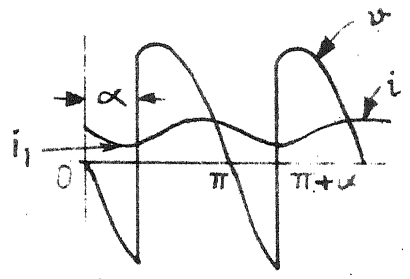

(a)

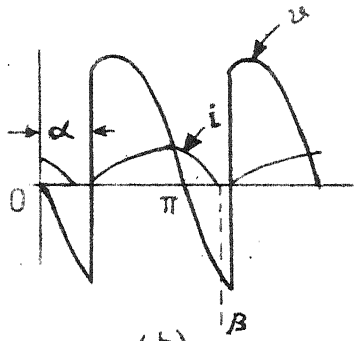

(b)

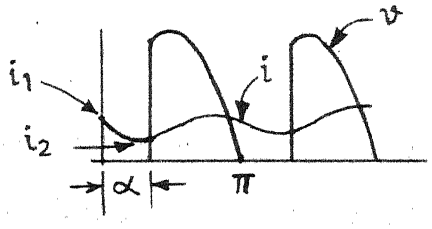

(c)

Fig. 3.1 Modes of operation

As far as calculation of speed-torque-current curves under continuous conduction for both fully-controlled and half-controlled converters is concerned, it does not make much difference in the final results whether approximation I, II or III is used. Therefore, for speed-torque-current curves under continuous conduction approximation I has been used.

3.2 Performance calculation when fed by fully-controlled converter:

A fully-controlled converter fed d.c. series motor normally operates in the following two modes, referring to Fig. 3.1.

(a) Continuous conduction mode: Fig. 3.1(a)

The basic equation governing this mode is given as

$$Em \sin wt = Ri + Lpi + E \quad \text{for } \alpha \leq wt \leq (\pi + \alpha) \qquad (3.1)$$

Assuming $E = K.W_{av}$, using approximation I and taking average of either side of equation (3.1), one gets,

$$\frac{2Em}{\pi} \cos\alpha = R\, I_{av} + KW_{av}$$

or

$$W_{av} = \left(\frac{2Em}{\pi} \cos\alpha - R\, I_{av} \right) . \frac{1}{K} \qquad (3.2)$$

and $T_{av} = K I_{av}$ (3.3)

As stated earlier, K is assumed to be a function of i_{av} rather than that of the instantaneous value i.

(b) Discontinuous conduction mode:

Referring to Fig. 3.1(b), the basic equations are:

$$Em \sin wt = Ri + Lp\, i + E \quad \text{for } \alpha \leq wt \leq \beta \tag{3.4}$$

$$\text{and } i = 0 \quad \text{for } \beta \leq wt \leq \pi + \alpha \tag{3.5}$$

For calculation of current zero, instantaneous expression of current has to be used, hence approximation I cannot be used without loss of accuracy. Since discontinuous conduction occurs at low values of current, the operating point lies in the linear part of the magnetisation characteristic. Therefore, approximation II with constant value of M_{af} corresponding to linear part has been employed in the calculation of performance. Thus

$$E = M_{af}\, i\, W_{av} \tag{3.6}$$

Then equation (3.4) has the solution

$$i(t) = \frac{Em}{Z} \sin(wt - \phi) + A \exp(-k_1 t) \tag{3.7}$$

where $Z = L(k_1^2 + w^2)^{1/2}$

and $\phi = \tan^{-1}(w/k_1)$

A is determined from the initial condition: i=0 at $t = \alpha/w$. Substituting for A,

$$i(t) = \frac{Em}{Z}(\sin(wt-\phi)-\sin(\alpha-\phi)\exp((-k_1/w)(wt-\alpha))) \quad (3.8)$$

For a given α , the critical speed W_c at which the discontinuous conduction just occurs, is given by the condition $\phi=\alpha$, since from the above equation it is seen that $i/_{wt=\pi+\alpha} = 0$ if $\phi = \alpha$.

From equation (3.8), putting i=0 at $wt = \beta$, one obtains

$$\sin(\beta-\phi)= \sin(\alpha-\phi)\exp(-(k_1/w)(\beta-\alpha)) \quad (3.9)$$

This equation is nonlinear in β and can be solved numerically, say by Bisection-Method.

Taking average of either side of equation (3.4) yields

$$I_{av} = \frac{Em}{\pi} \frac{(\cos\alpha - \cos\beta)}{R+M_{af} W_{av}} \quad (3.10)$$

and $$T_{av} = M_{af} I_{av}^2 \quad (3.11)$$

Now the speed-torque characteristics can be determined as follows:

(i) For a given α, corresponding to $W_{av}(> W_c)$, the value of β is determined from equation (3.9).

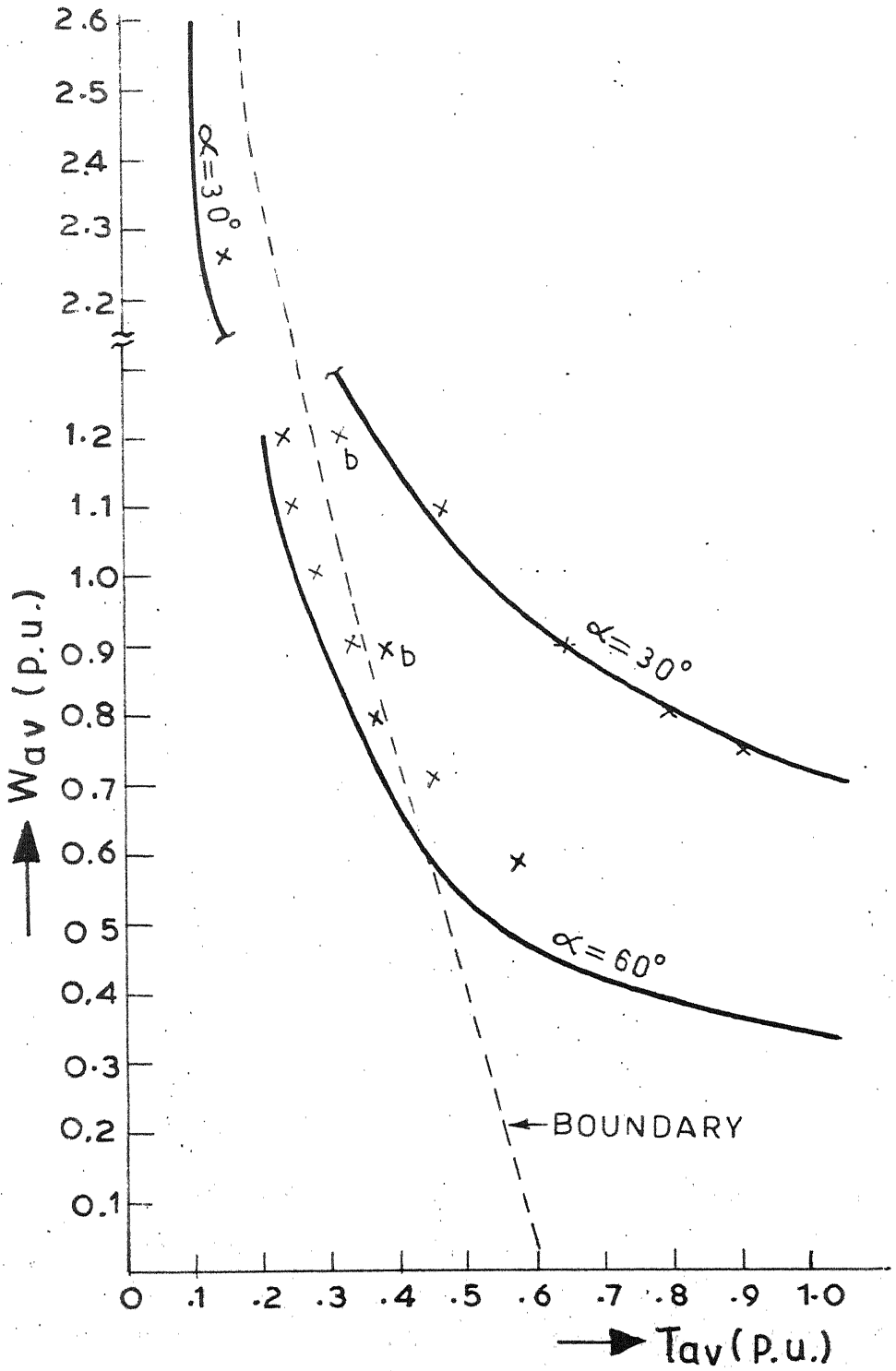
2.6
2.5
2.4
2.3
2.2
1.2
1.1
1.0
0.9
0.8
0.7
0.6
0.5
0.4
0.3
0.2
0.1
W_{av} (p.u.)
$\alpha = 30°$
b
b
$\alpha = 30°$
$\alpha = 60°$
BOUNDARY
0
.1
.2
.3
.4
.5
.6
.7
.8
.9
1.0
T_{av} (p.u.)

FIG.3.2

ii) The I_{av} is calculated from equation (3.10) and hence T_{av} can be calculated from equation (3.11),

iii) The critical value of I_{av}, i.e. I_c corresponding to W_c, is known from equation (3.10).

iv) The $I_{av}(> I_c)$ is assumed and the corresponding value of K is obtained from magnetisation characteristic.

v) W_{av} and T_{av} are then calculated from equations (3.2) and (3.3) respectively.

A set of characteristics is shown in Fig. 3.2.

The ripple factor in the armature current is defined as

$$CRF = \frac{i_{max} - i_{min}}{2}$$

since the performance equations for ripple involve instantaneous value of current, approximation I cannot be used. It's found that approximation III results in better accuracy of ripple, hence it has been made use of in calculating ripple.

For the case of fully-controlled converter feeding the motor, the ripple can be calculated as follows:

Referring to Fig. 3.1(a), the basic equation governing the operation is given by

$$Em \sin wt = Ri + Lp\, i + E$$

where, using approximation III,

$E = (C_o + C_1 i) W_{av}$, the values of C_o and C_1 being dependent on the value of I_{av}, i.e., the operating point.

In appendix I, it is shown that

$$i(t) = Im(\sin(wt-\phi) - \sin(\alpha-\phi) e^{A(\alpha - wt)/w}) - \frac{C_o W_{av}}{A.L} \cdot (1 - e^{-A(wt-\alpha)/w}) + i_1 e^{-A(wt-\alpha)/w}$$

The various symbols appearing in the above equation are defined in the appendix I.

For a given value of α and I_{av}, the maximum and minimum values of current can be calculated from the above equation.

3.3 Performance prediction when fed by half-controlled converter:

Referring to Fig. 3.1(c), the performance of the d.c. series motor fed by half-controlled converter can be described by the following equations:

Duty interval ($\alpha \leq wt \leq \pi$)

$$Em \sin wt = R i + L pi + E \qquad (3.12)$$

Free wheeling interval ($\pi \leq wt \leq \pi + \alpha$)

$$0 = R i + L pi + E \qquad (3.13)$$

where E is again given by $E = K(i_{av})W_{av}$.

K being a function of current, equations (3.12) and (3.13) are nonlinear differential equations and can be solved numerically using 4th order R-K method or predictor-corrector method. However, the computation time is very large.

To compute the performance from the equations (3.12) and (3.13) with much less computation time and with fairly good accuracy, K is assumed to be a function of average value of current during the cycle rather than that of instantaneous value of current. Then taking average of either sides of equations (3.12) and (3.13), one gets using approximation I,

$$\frac{Em}{\pi}(1 + \cos\alpha) = RI_{av} + K.W_{av}$$

or $$W_{av} = \left(\frac{Em}{\pi}(1+\cos\alpha) - RI_{av}\right)/K \qquad (3.14)$$

and $$T_{av} = K\, I_{av} \qquad (3.15)$$

The speed-torque characteristics are then evaluated in following two steps:

(i) For a given α, I_{av} is assumed and the corresponding value of K is obtained from the magnetisation characteristic.

(ii) W_{av} and T_{av} are then calculated from equations (3.14) and (3.15) respectively.

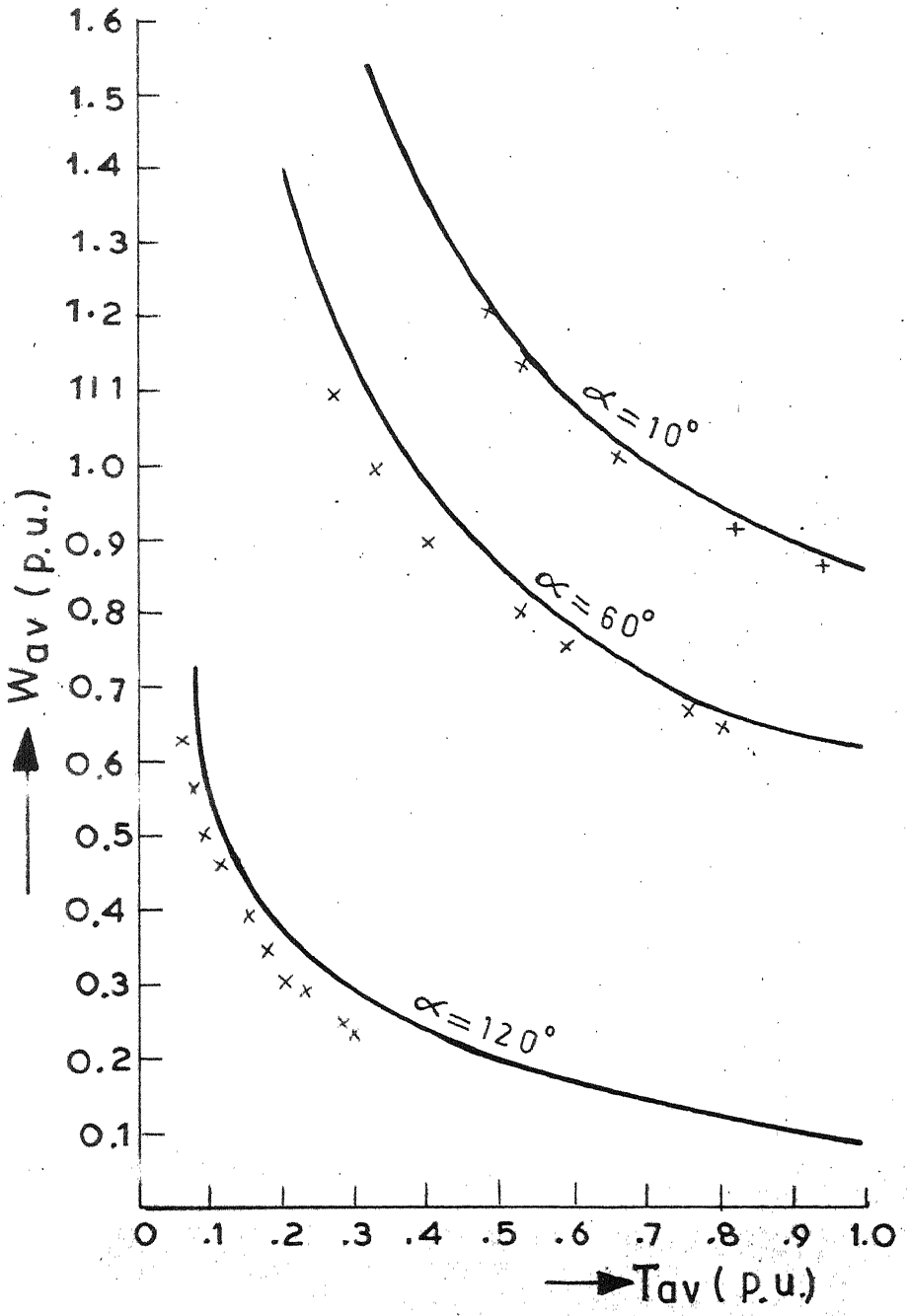
1.6
1.5
1.4
1.3
1.2
1.1
1.0
0.9
0.8
0.7
0.6
0.5
0.4
0.3
0.2
0.1
Wav (p.u.)
α=10°
α=60°
α=120°
0
.1
.2
.3
.4
.5
.6
.7
.8
.9
1.0
Tav (p.u.)

FIG. 3.3

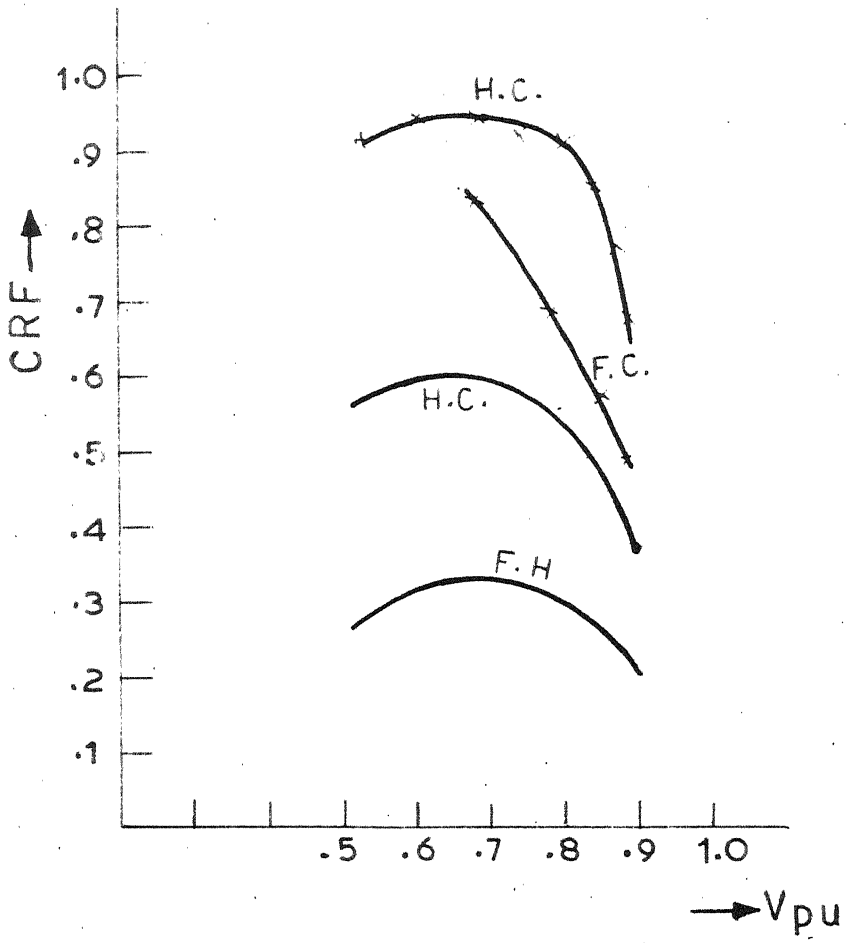

Fig. 3.4 Variation of CRF with input voltage

A set of computed characteristics is shown in Fig. 3.3.

Referring to Fig.3.1(c), the CRF can be calculated by solving equations (3.12) and (3.13) in conjunction with the approximation III, i.e., $E=(C_0+C_1 i)W_{av}$, which yield

$$i = i_f = -C+D(1-e^{-A\pi/w})^{-1} \; e^{-At} \quad \text{for} \quad 0 \leq wt \leq \alpha$$

and

$$i = i_d = I_m(\sin(wt-\phi)-\sin(\alpha-\phi)e^{-A(wt-\alpha)/w})+D(1-e^{-A\pi/w})^{-1}$$

$$e^{-At} - C$$

The derivation of equations and various constants are given in appendix I. The CRF can be determined from these equations for a given values of α and I_{av}.

A plot of CRF vs. V_{pu} for a given value of I_{av} is shown in Fig. 3.4 for both fully-controlled and half-controlled converters.

3.4 Calculation of filter inductance:

In a d.c. drive, the discontinuous conduction and associated large a.c. ripple are not desirable as they affect the commutation, regulation and efficiency of the drive. The discontinuous conduction can be eliminated by adding inductance to the armature circuit. However, increase in the armature circuit inductance is not desirable from

other points of views, such as increase in losses, cost, weight and deterioration of transient response. Hence, the value of the external inductance to be added should be just sufficient to eliminate the discontinuous conduction and keep the a.c. ripple within acceptable limits. In this section, a method is presented for calculating the optimum value of filter inductance.

(a) Performance equations:

As discussed in Section 3.2, the equations from which the critical value of speed, W_c and the corresponding value of torque, T_c, for a given value of α, are derived, are given as follows:

$$\alpha = \phi = \tan^{-1} (wL/(R+M_{af} W_c)) \qquad (3.16)$$

and

$$I_c = \frac{2 Em}{\pi} \frac{\cos\alpha}{(R+M_{af}W_c)} \qquad (3.17)$$

and $$T_c = K(I_c).I_c \qquad (3.18)$$

The value of $\phi > \alpha$ results in continuous conduction and $\phi \leq \alpha$ results in discontinuous conduction.

Eliminating α from (3.16) and (3.17),

$$2 \frac{Em}{\pi} / (R+M_{af} W_c)(1+(wL/(R+M_{af} W_c)^2)^{1/2}) = I_c$$

or

$$\frac{2\,Em}{\pi R} / ((1+M_{af}\,W_c/R)^2 + (wT_a)^2)^{1/2} = I_c$$

Squaring both sides,

$$1/((1+M_{af}\,W_c/R)^2+(\,wT_a\,)^2)=(I_c/I_R)^2 = T_p$$

$$\text{where } I_R = 2\,Em/\pi\,R$$

$$\text{or, } 1/((1+W_p)^2 + (\,wT_a)^2) = T_p \qquad (3.19)$$

Equation (3.19) gives boundary between continuous and discontinuous conduction on normalised speed and normalised torque plane for a given value of T_a, the armature circuit time constant. A set of boundaries computed for various values of T_a are shown in Fig. 3.5 . Area to the left of the boundaries represent discontinuous conduction.

(b) Selection of filter inductance:

Since series motor is not expected to run under no load, the minimum values of developed torque for various speeds are obtained from the requirement of the load to be driven by the motor and then plotted on the · normalised plane, as shown in Fig. 3.5. For the discontinuous conduction to be absent, the value of T_a should be such that the boundary lies to the left of this curve.

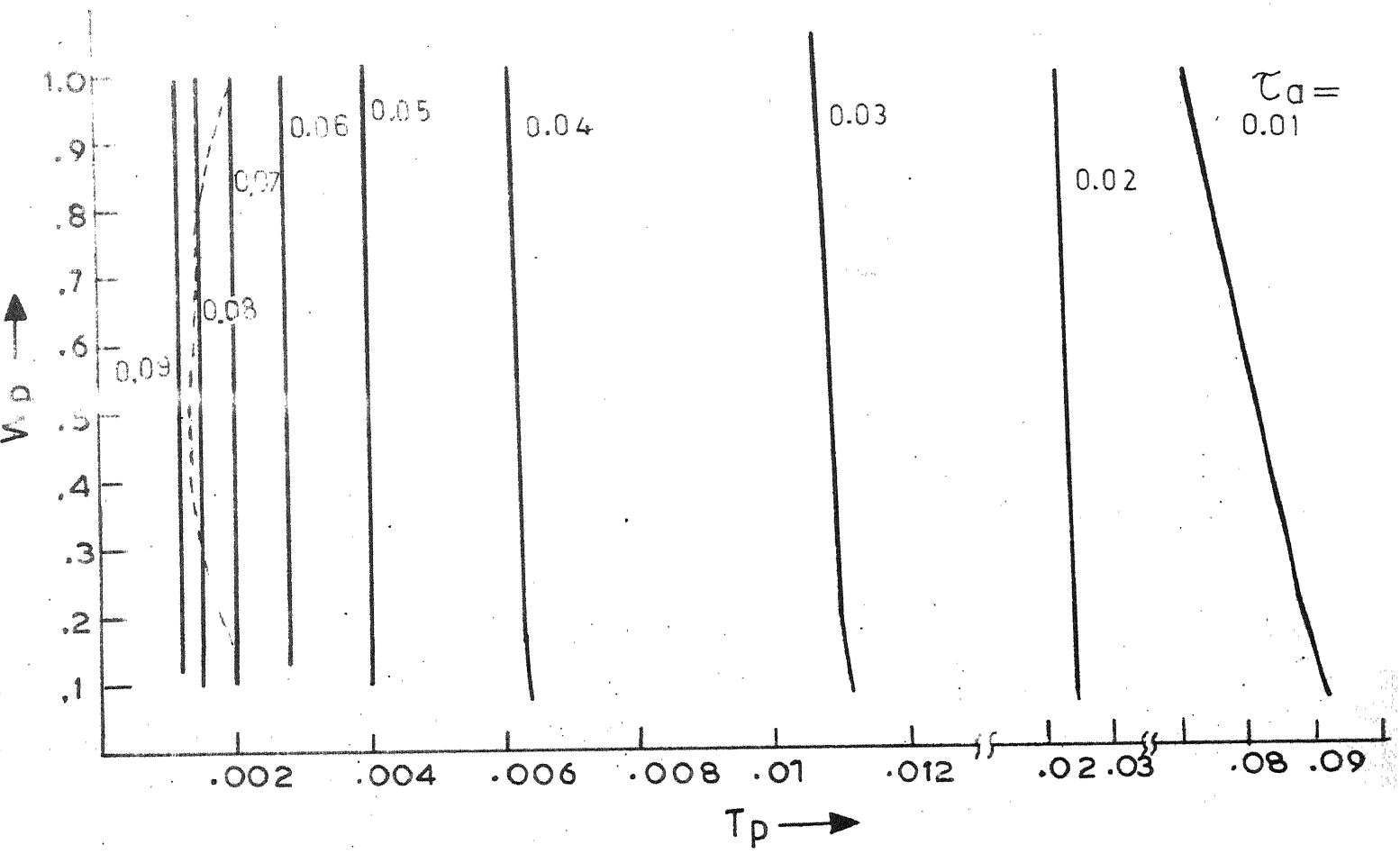

Fig. 3.5 Normalised boundaries

After the value of T_a is chosen, the maximum value of ripple is calculated to check whether it is within permissible limits or not. If it is not,one should try larger value of T_a. Then the value of additional inductance is calculated.

3.5 Experimental verification:

For a fixed value of firing angle α, the motor speeds and the corresponding load torques are measured. A set of speed-torque characteristics thus measured for various values of firing angles are shown in Fig. 3.2 and Fig. 3.3 respectively for the cases of fully-controlled and half-controlled converters. As firing angle is varied, the critical speed and critical torque at which just continuous conduction takes place, are measured to obtain the boundary between continuous and discontimuous conduction as shown by X_b in Fig. 3.2. The theoretically computed speed-torque characteristics and boundary are also shown in the figures. There is a satisfactory agreement between experimental and predicted results.

For a fixed value of load-torque and hence the load-current, the ripple in the armature current is measured for various values of firing angles, by measuring the maximum and minimum values of current, and CRF vs. V_{pu} have been plotted in Fig. 3.4 along with the computed ones.

CHAPTER 4

TRANSIENT ANALYSIS OF CONVERTER-CONTROLLED D.C. SERIES MOTOR

4.1 Introduction:

A half-controlled converter fed d.c. series motor normally operates in two modes, namely the duty interval and free wheeling interval, during a cycle. The performance of the motor can be described by the following equations, referring to Fig. 3.1(c).

Duty interval ($\alpha \leq wt \leq \pi$)

$$Lpi = Em \sin wt - R\,i - K(i)W \qquad (4.1)$$

Also, from motor-load dynamics

$$J\,pW = K(i) - BW - T_L \qquad (4.2)$$

Freewheeling interval ($0 \leq wt \leq \alpha$)

$$L\,pi = -R\,i - K(i)\,W \qquad (4.3)$$

and

$$JpW = K(i) - BW - T_L \qquad (4.4)$$

The performance equations for the fully-controlled converter case are given by

$$Lpi = Em \sin wt - Ri - K(i)W \text{ for } \alpha \leq wt \leq (\pi + \alpha) \qquad (4.5)$$

and

$$J\,p\,W = K(i) - BW - T_L \qquad (4.6)$$

In the above equations, K(i) represents K as a function of the instantaneous value of motor current, so that the equations represent a set of simultaneous nonlinear differential equations.

One way to calculate the transient response is to solve the above equations numerically, for each converter cycle using the final conditions of the previous cycle as the initial conditions for each successive cycle. The advantage of this approach is that it permits the calculation of transient response exactly for the assumed model. However, the computation time involved is rather large, particularly for systems with slow transient response.

In this chapter have been given two new methods for the fast calculation of the transient response. These methods can also be employed for deriving the small signal transfer function of the converter controlled d.c. series motor around a steady-state point, which can be used in the dynamic response analysis of the closed-loop system incorporating a d.c. series motor controlled by converter. The transient response obtained from these two methods has

been compared with that obtained from exact method as well as with that measured experimentally.

Whereas discontimuous conduction has been ignored in case of half-controlled converter,due consideration has been given to this in case of fully-controlled converter. The assumption that the converter cycle time is usually small compared with mechanical time constant of the motor, has been made throughout. The prediction of transient response has been confined to the variation of average values of current and speed, rather than the instantaneous values.

4.2 Transient analysis when the motor is fed by fully-controlled converter:

Method I: First-order model.

Assuming that the mechanical time constant of the motor is fairly large compared with the supply period and the armature circuit time constant, we get, taking average of either sides of equations (4.5) and (4.6), using approximation I,

$$V_{av} = R\, i_{av} + uK\, W_{av}$$

or

$$i_{av} = \frac{V_{av} - uK\, W_{av}}{R} \qquad (4.7)$$

where $V_{av} = \frac{2Em}{\pi} \cos \alpha$

and u is the fraction of half cycle for which the armature current flows continuously. Thus u = 1 for continuous conduction. And

$$J\ pW_{av} = K\ i_{av} - BW_{av} - T_L \qquad (4.8)$$

(i) Continuous conduction:

Here u = 1, so that from equations (4.7) and (4.8) one gets,

$$i_{av} = \frac{V_{av} - KW_{av}}{R} \qquad (4.9)$$

and

$$J\ pW_{av} = K\ \left(\frac{V_{av} - KW_{av}}{R}\right) - B.W_{av} - T_L$$

or

$$pW_{av} + ((K^2 + R.B)/JR)W_{av} = (K.V_{av} - R.T_L)/J.R \qquad (4.10)$$

This equation, though nonlinear, can be solved by piecewise linear approximation as follows:

Values of i_{av} and W_{av} at the beginning of the transient will be known. A suitable iteration interval is chosen. The value of K during this interval is assumed to be constant at a value corresponding to the value of i_{av} at the beginning of the interval, using approximation I of Fig. 2.3(a). This makes equation (4.10) linear during this interval. The

value of W_{av} at the end of this interval is obtained from equation (4.10). The corresponding value of i_{av} is then obtained from equation (4.9).

If the transient response is calculated by solving equations (4.5) and (4.6) by point-by-point method, the numerical computations must be done for small increments of time in each cycle, thus requiring a large number of computations for each cycle. In the above approximate method, equation (4.10) can be solved by piecewise linear approximation by choosing the time of iteration as large as 10 cycles without introducing appreciable error. Thus, the computation time is reduced by large amount. Here it is assumed that the motor starts only after its developed torque exceeds the load torque.

The transient response for small signal perturbations around a steady-state point can also be derived from equation (4.10) using approximation I.

Let the steady-state operating-point be (α_o, W_{avo}, T_L, I_{avo}). Let the incremental changes in these variables due to a disturbance be denoted by $\Delta\alpha$, ΔW_{av}, Δi_{av} and ΔT_L. Then using the approximation I, i.e., $K=K_o$ for increments in i_{av}, equation (4.8) becomes

$$Jp\ (W_{avo}+\Delta W_{av})=K_o(I_{avo}+\Delta i_{av})-B(W_{avo}+\Delta W_{av})-(T_L+\Delta T_L)$$

which simplifies to

$$Jp\ (\Delta W_{av}) = K_o\ \Delta i_{av} - B.\ \Delta W_{av} - \Delta T_L \qquad (4.11)$$

From equation (4.9),

$$\Delta i_{av} = (V'_{avo}(\alpha)\ \Delta\alpha - K_o \cdot \Delta W_{av})/R,$$

$$\text{where } V'_{avo}(\alpha) = -2\,\frac{Em}{\pi}\ \sin\alpha_o$$

Substituting in equation (4.11),

$$Jp\ (\Delta W_{av}) = -\left(\frac{K_o^2}{R} + B\right)\Delta W_{av} + \frac{K_o}{R} \cdot \frac{V'_{avo}(\alpha)}{\Delta\alpha} - \Delta T_L$$

or,

$$T_{m2}\ p(\Delta W_{av}) + \Delta W_{av} = + \frac{K_o \cdot V'_{avo}(\alpha).\ \Delta\alpha}{(K_o^2 + R.B)} - \Delta T_L \cdot \frac{T_{m2}}{J}$$

Laplace transforming,

$$T_{m2} \cdot s \cdot \Delta W_{av}(s) + \Delta W_{av}(s) + K_m \cdot \Delta\alpha(s) + \frac{T_{m2}}{J} \cdot \Delta T_L(s) = 0 \qquad (4.12)$$

where,

$$T_{m2} = \frac{J.R}{K_o^2 + R.B} \quad \text{and} \quad K_m = -\frac{T_{m2}}{JR}\, K_o \cdot V'_{avo}(\alpha)$$

For $\Delta T_L = 0$,

$$\frac{\Delta W_{av}(s)}{\Delta\alpha(s)} = -\frac{K_m}{1 + sT_{m2}} \qquad (4.13)$$

and, for $\Delta\alpha = 0$,

$$\frac{\Delta W_{av}(s)}{\Delta T_L(s)} = -\frac{T_{m2}}{J(1+sT_{m2})} \qquad (4.14)$$

Similarly the variation of current can be determined. Equations (4.13) and (4.14) show that this is a first-order approximation to a system which is actually of second-order.

The block diagram for small perturbations is shown in Fig. 4.1.

(ii) Discontinuous conduction.

In this case, $u < 1$. From equations (4.7) and (4.8),

$$Jp\, W_{av} = K(V_{av} - uK\, W_{av})/R - B\, W_{av} - T_L$$

or,

$$pW_{av} + (K^2 u + B.R)W_{av}/JR = (K\, V_{av} - RT_L)/JR \qquad (4.15)$$

$u\,(=\beta/\pi)$ being a function of W_{av}, its values corresponding to speeds $W_{av}(> W_c)$ are calculated as in Section 3.2(b), and transient response is calculated by piecewise linear approximation as described earlier.

Method II: Second-order model.

(i) Continuous conduction.

For nth cycle, from equations (4.5) and (4.6),

$$(w/\pi)\int_{i_{d1}(n)}^{i_{d1}(n+1)} di(n)=(1/L)((Em/\pi)\int_{n\pi}^{(n+1)\pi}\sin wt\,d(wt)$$

$$-(K\,w/\pi)\int_{n\pi/w}^{(n+1)\pi/w} W(n)\,dt-(\frac{Rw}{\pi})\int_{n\pi/w}^{(n+1)\pi/w} i(n)dt$$

and,

$$(w/\pi)\int_{W_{d1}(n)}^{W_{d1}(n+1)} dW(n)=(1/J)((Kw/\pi)\int_{n\pi/w}^{(n+1)\pi/w} i(n)dt-(B\,w/\pi)$$

$$\int_{n\pi/w}^{(n+1)\pi/w} W(n)dt\ -(T_L\cdot w/\pi)\int_{n\pi/w}^{(n+1)\pi/w} dt$$

Simplifying,

$$p\ i_{av}(n)=(i_{d1}(n+1)-i_{d1}(n))/T=(V_{av}-K.W_{av}(n)-Ri_{av}(n))/L \qquad (4.16)$$

and

$$p\ W_{av}(n)=(W_{d1}(n+1)-W_{d1}(n))/T=(Ki_{av}(n)-B\,W_{av}(n)-T_L)/J \qquad (4.17)$$

where $T = \pi / w$

From above two equations, we get the following general relations.

$$p\, i_{av} = (V_{av} - K\, W_{av} - R i_{av})/L \tag{4.18}$$

and $$p\, W_{av} = (K i_{av} - B W_{av} - T_L)/J \tag{4.19}$$

Assuming K to be constant for small interval of time, separating i_{av} and W_{av} from the above two equations, one gets,

$$T_a\, p^2\, i_{av} + (1 + T_a/T_{m1})\, p\, i_{av} + i_{av}/T_{m2} = (V_{av} \cdot B + K T_L)/JR \tag{4.20}$$

and

$$T_a\, p^2\, W_{av} + (1 + T_a/T_{m1})\, p\, W_{av} + W_{av}/T_{m2} = (K V_{av} - R T_L)/JR \tag{4.21}$$

These are second-order nonlinear differential equations which can be solved by piecewise linear approximation as described earlier.

Using approximation I, the transient response for small perturbation around a steady-state point can be obtained as follows:

For small increments, from equations (4.18) and (4.19),

$$V'_{avo}(\alpha)\, \Delta\alpha(s) = (R + sL)\, \Delta i_{av}(s) + K_o\, \Delta W_{av}(s) \tag{4.22}$$

$$(B + sJ) \cdot \Delta W_{av}(s) = K_o \cdot \Delta i_{av}(s) - \Delta T_L(s) \tag{4.23}$$

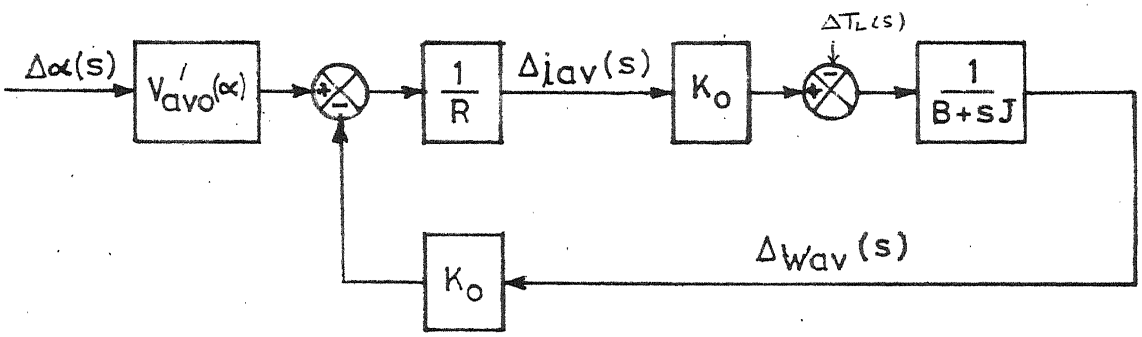

Fig. 4.1 First-order model

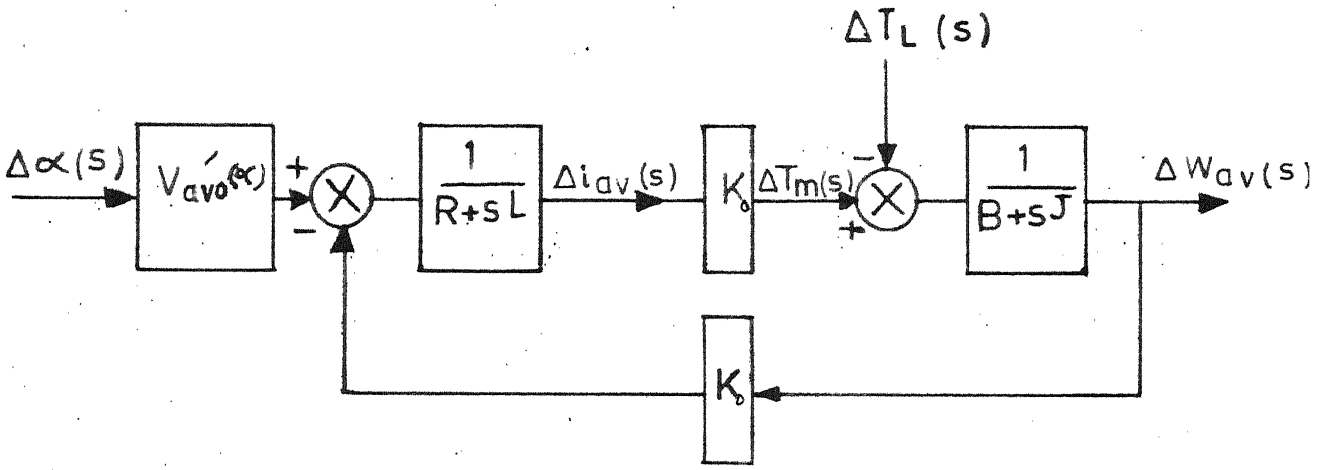

Fig. 4.2 Second-order model; closed Loop block diagrams of series motor for small perturbation

From the above two equations, a block diagram of the system can be obtained as shown in Fig. 4.2.

For $\Delta T_L = 0$,

$$\frac{\Delta W_{av}(s)}{\Delta \alpha (s)} = \frac{K_0 V'_{avo}(\alpha)/JL}{s^2+s(R/L+B/J)+(BR+K_0^2)/JL} \tag{4.24}$$

and

$$\frac{\Delta i_{av}(s)}{\Delta \alpha (s)} = \frac{V'_{avo}(\alpha)(B+sJ)/JL}{P(s)} \tag{4.25}$$

and for $\Delta \alpha = 0$,

$$\frac{\Delta W_{av}(s)}{\Delta T_L(s)} = \frac{(R+sL)/JL}{P(s)} \tag{4.26}$$

and,

$$\frac{\Delta i_{av}(s)}{\Delta T_L(s)} = \frac{K/JL}{P(s)} \tag{4.27}$$

where $P(s) = s^2+s(R/L+B/J)+(BR+K_0^2)/JL$

(ii) Discontinuous conduction.

Assuming K to be constant at a value corresponding to the value of i_{av} during the iteration interval, equations (4.18) and (4.19) become

$$L\ p\ i_{av} = V_{av} - R\ i_{av} - \mu K\ W_{av} \tag{4.28}$$

and

$$J\ p\ W_{av} = K i_{av} - B\ W_{av} - T_L \tag{4.29}$$

Assuming $p\,u \to o$, we get on differentiating (4.28)

$$L\,p^2\,i_{av} = -R\,pi_{av} - uK\,pW_{av}$$

Substituting for pW_{av} and W_{av} from equation (4.29) and rearranging the terms, one gets

$$T_a\,p^2\,i_{av} + (1+T_a/T_{m1})\,p\,i_{av} + i_{av}/T_{m21} = K_2/T_{m2} \qquad (4.30)$$

where

$$T_{m1}=J/B,\ T_{m21}=JR/(uK^2+BR) \text{ and } K_2 = T_{m21}(uK\,T_L+BV_{av})/JR$$

Similarly, differentiating equation (4.29) with the same assumption that $p\,u \to o$, one obtains

$$T_a\,p^2\,W_{av} + (1+T_a/T_{m1})\,p\,W_{av} + W_{av}/T_{m21} = K_1/T_{m21} \qquad (4.31)$$

where $K_1 = T_{m21}\,(K\,V_{av} - T_L\,R)/JR$

The transient response is calculated from equations (4.30) and (4.31) as explained earlier by piecewise linear approximation.

4.3 Transient analysis when motor is fed by half-controlled converter:

In the transient analysis, the expressions for methods I and II remain exactly the same as for fully-controlled converter with continuous conduction. Only the value of V_{av} and V'_{avo} change. They become

$$V_{av} = \frac{Em}{\pi}(1+\cos\alpha) \text{ and } V'_{avo}(\alpha) = -\frac{Em}{\pi}\sin\alpha_{o}.$$

4.4 Experimental Verification:

The transient response for various values of firing angles and load torques are recorded and have been plotted along with the computed results in Figure 4.3, 4.4 and 4.5 since for carrying out experiments the coupled generator load has been used, the constant load torque T_L used in various basic equations has been replaced by

$$T_L = K'W$$

where K' is the load torque proportionality constant. It is seen that there is fairly good agreement between the computed and experimentally obtained results. To examine the accuracy of methods I and II, the results computed by these methods have been plotted along with those obtained by step-by-step method, since this permits the calculation of transient response exactly for an assumed model. It is observed that method II gives results which are quite close to those obtained by step-by-step method. Method I is grossly inaccurate, particularly in the prediction of current/time curve, since it uses a first-order approximation of a second-order system.

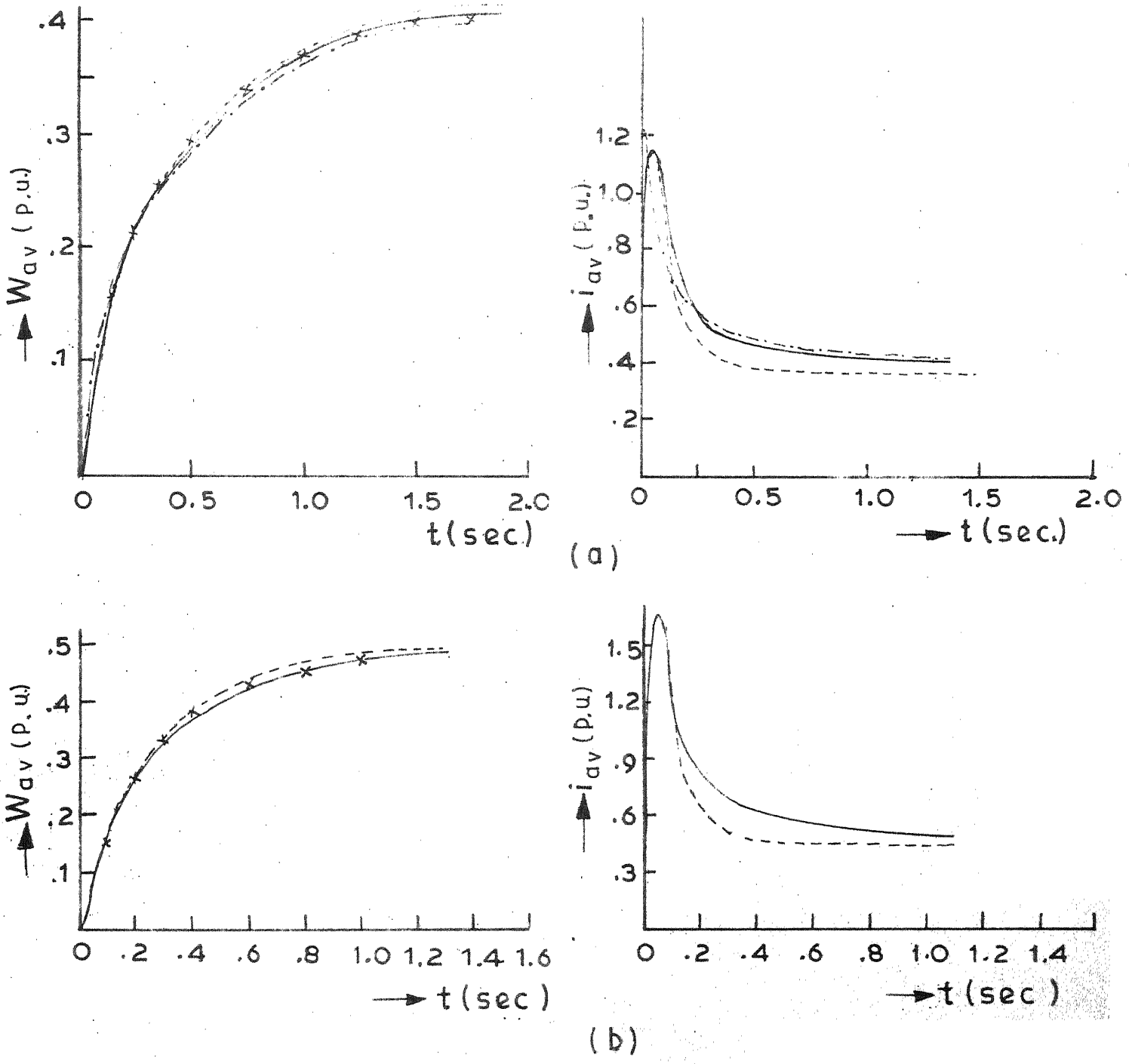

Fig. 4.3 Transient response for half-controlled converter fed d.c. series motor

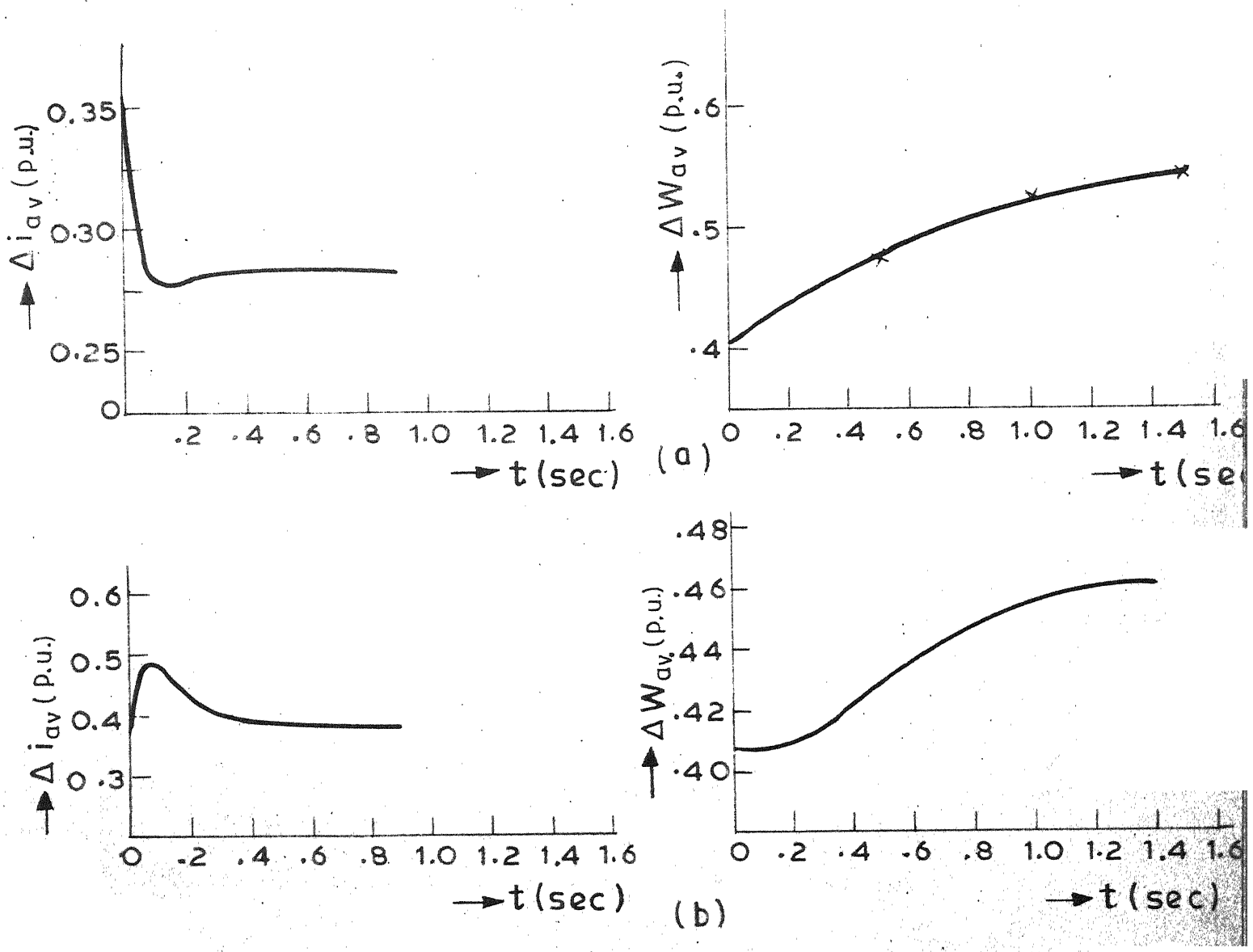

Fig. 4.4 Transients for small perturbations

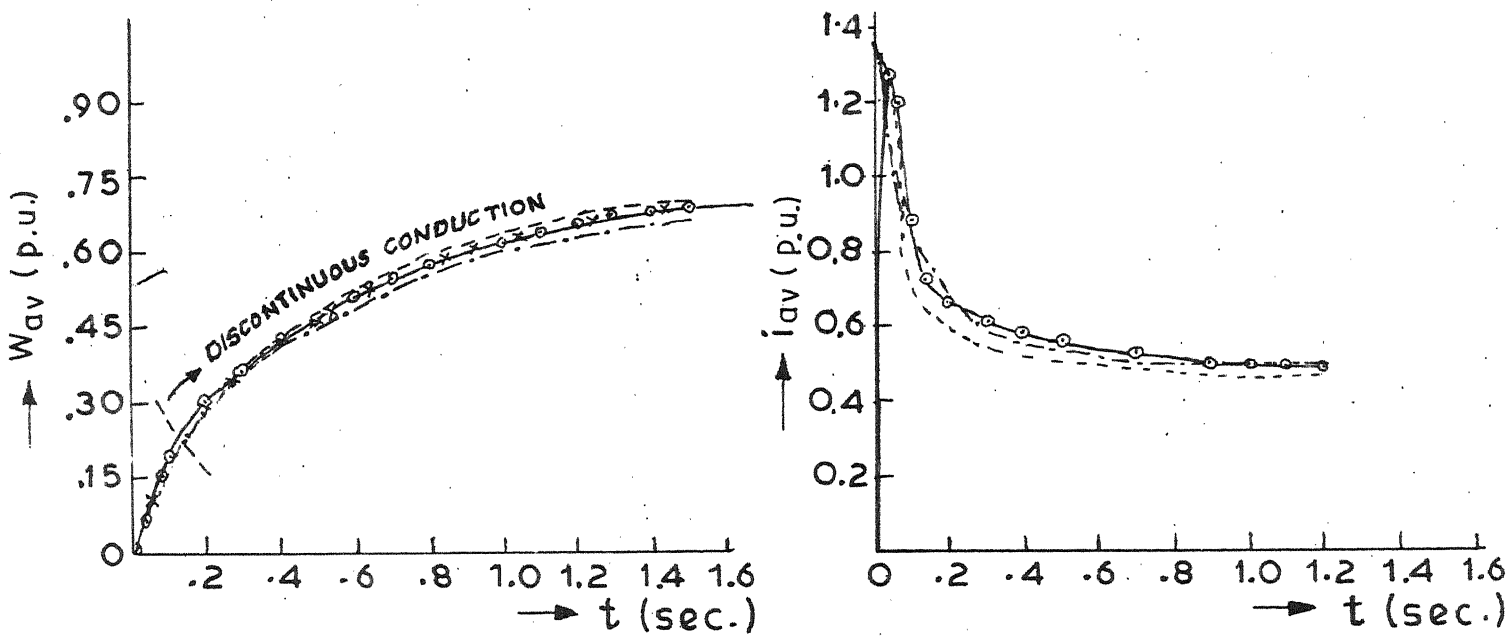

Fig.4.5 Transient response for fully controlled converter fed series motor

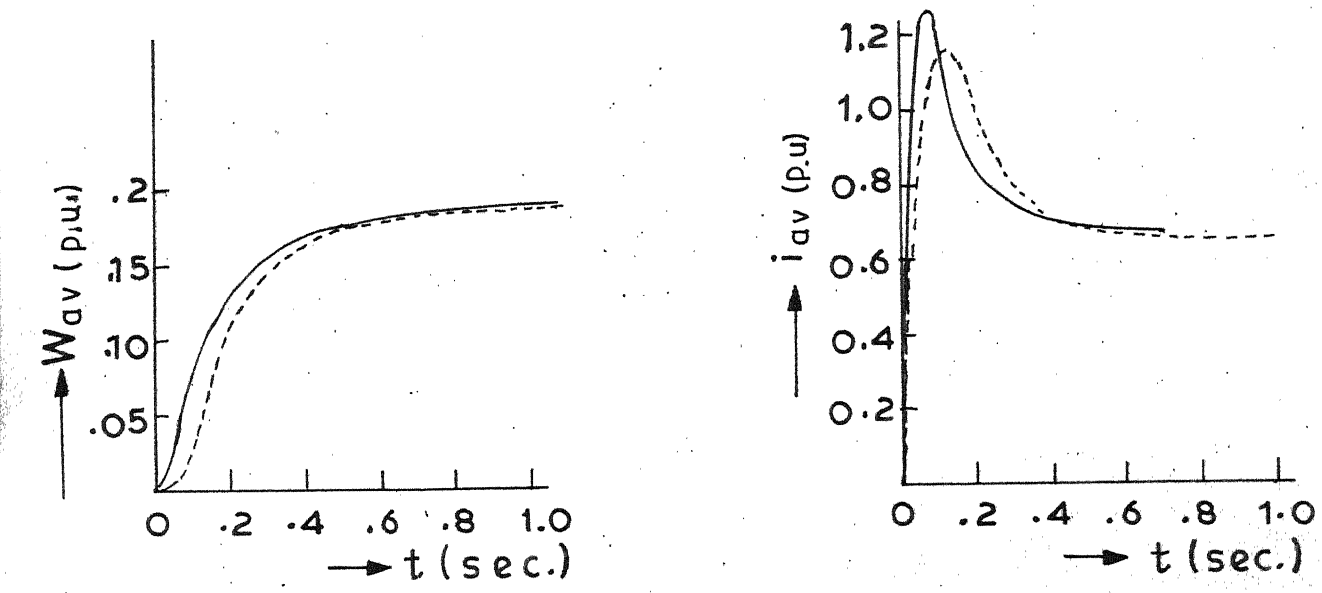

Fig. 4.7 Effect of inductance

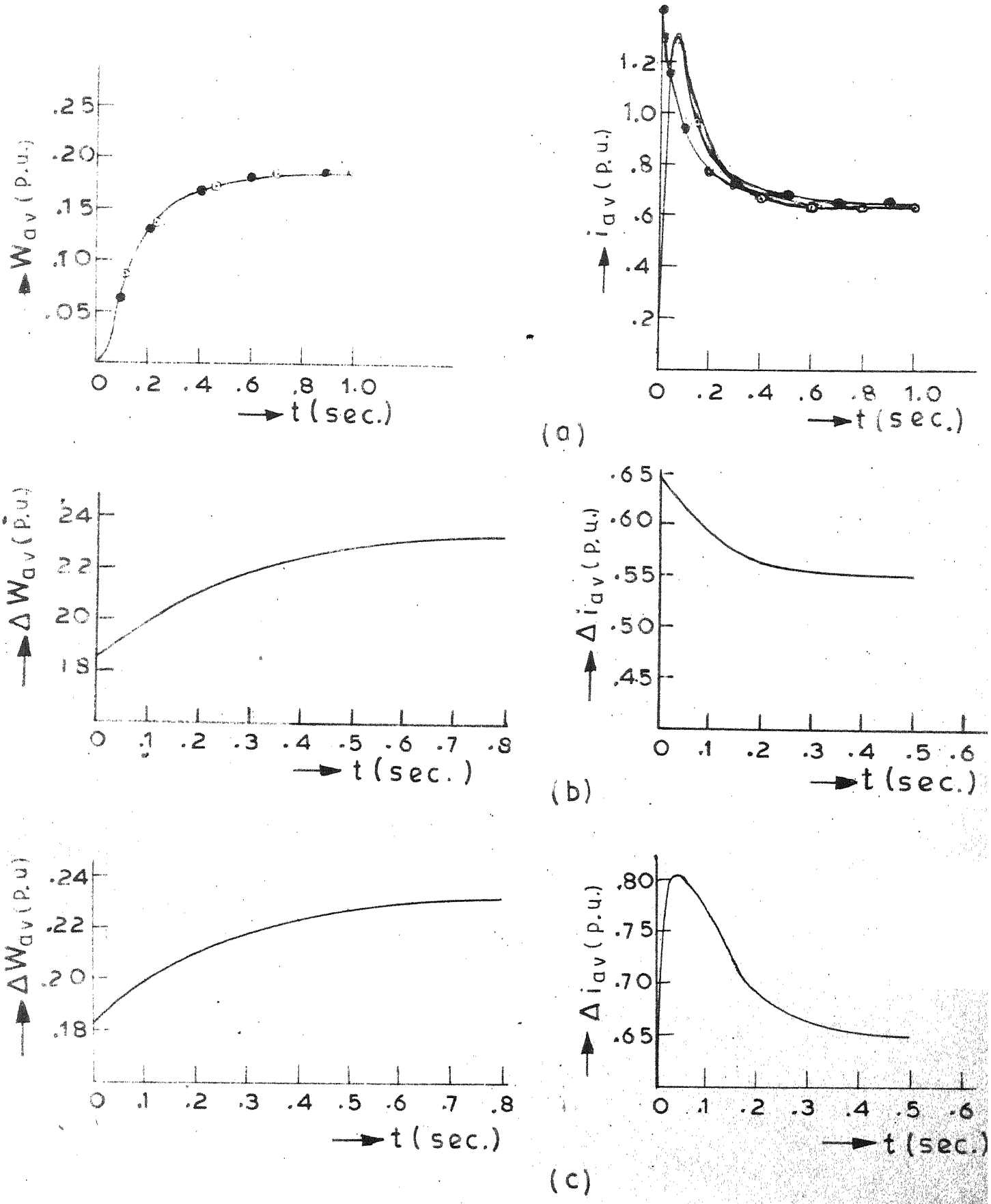

Fig.4.6 Transient response when fed by half-controlled converter with constant T_L

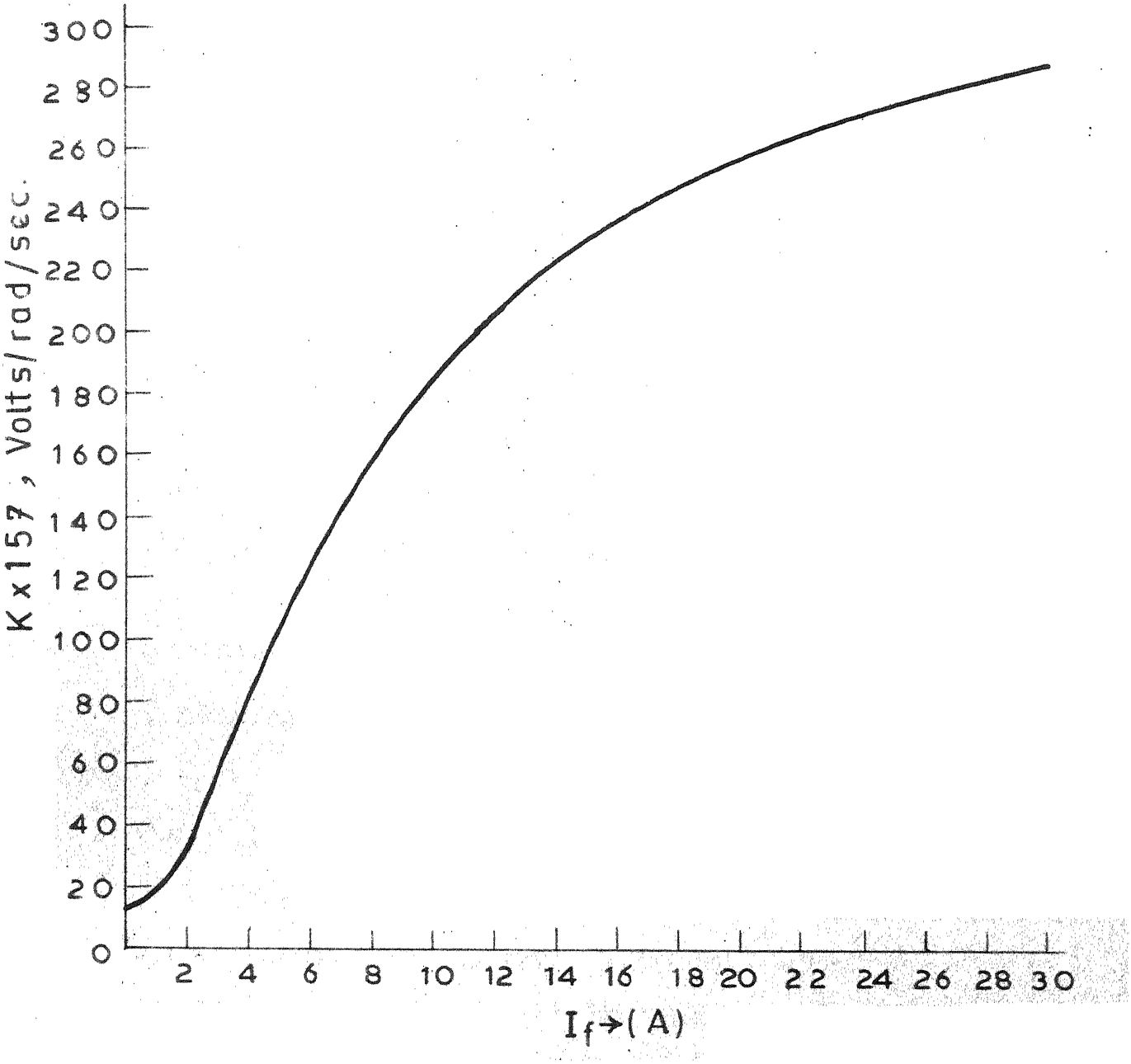

Fig. 4.8 Magnetisation characteristic

CHAPTER 5

A FIRING CIRCUIT FOR VARIOUS METHODS OF CONVERTER CONTROL

5.1 Introduction:

A firing circuit proposed by Anjaneyulu [10] has been fabricated. This circuit is simple and versatile in that it can be conveniently used for many converter operations such as i) fully-controlled operation, ii) fully-controlled operation with half-controlled characteristics iii) sequence control, iv) symmetrical pulse width modulation with one pulse per half cycle and v) asymmetrical triggering control. The same principle can be extended to 3-phase a.c. voltage controller and 3-phase thyristor bridge converter operation. This circuit is stable and immune to stray pulse and noise unlike those using monostable circuits.

5.2 Firing scheme:

A block diagram of the firing scheme is shown in Fig. 5.1. The basic waveforms are given in Fig. 5.3.

The principle of operation is based on converting the synchronisation supply (Fig. 5.3a) to a square wave. A triangular wave TR1 (Fig. 5.3d) is generated by integrating the square wave. TR1 is compared with reference voltage

V_{ref} to generate a pulse B of duration α to $2\pi - \alpha$ as shown in in Fig. 5.3(e). TR1 is also inverted and compared with reference voltage V_{ref}. The pulse C of duration $\pi - \alpha$ to $\pi + \alpha$ is obtained as shown in Fig. 5.3(g). The pulse A (Fig. 5.3a) is obtained separately by chopping the negative part of the square wave. The pulses A,B and C can now be processed to get the pulses of any of the following duration: (1) 0 to π, (2) π to 2π, (3) α to π, (4) $\pi - \alpha$ to π, (5) $\pi + \alpha$ to 2π, (6) $2\pi - \alpha$ to 2π, (7) α to $\pi - \alpha$, (8) $\pi + \alpha$ to $2\pi - \alpha$. This makes the circuit suitable of adoption to any converter control mentioned above.

5.3 Realisation:

The circuit diagram is shown in Fig. 5.2. Dual OPAMPs have been used in fabrication. The waveforms at the output of each stage have been shown in Fig. 5.3. OP-1 converters the synchronisation supply to a square wave. OP-2 integrates this. Any d.c. level introduced at the output (Fig. 5.3c) may be adjusted to obtain waveform as shown in Fig. 5.3(d) by a d.c. level shifter OP-3. This is compared with reference voltage V_{ref} and the wave form as shown in Fig. 5.3(e) is obtained. The wave form TR1 (Fig. 5.3d) is inverted and level-shifted by OP-5 to obtain wave form of Fig. 5.3(f). This is compared with reference voltage V_{ref} to obtain waveform C of Fig. 5.3(g). Wave form A is

Fig. 5.3(i). During negative half cycle, at instant π, thyristor T_3 is triggered by the waveform of Fig. 5.3(h) and part CD of waveform of Fig. 5.5(b) is obtained. At instant D, T_4 is triggered by the waveform of Fig. 5.3(k). The part EF of the waveform of Fig. 5.5(b) is obtained. The part GA is obtained by the triggering of thyristor T_1 by waveform of Fig. 5.3(b). Thus the circuit operates as a fully-controlled bridge with half-controlled characteristics.

(c) Sequence control:

The power circuit is shown in Fig. 5.4(b). The output voltage waveform E_{out} is shown in Fig. 5.5(c). The part AB of the waveform is obtained by the conduction of T_2 triggered by the waveform of Fig. 5.3(b) and by the diodes D_1, D_3, and D_4. At the instant α, T_4 is triggered by the waveform of Fig. 5.3(i) and the part CD is obtained. During the negative half cycle of the supply, at instant D, T_1 is triggered by the waveform of Fig. 5.3(h). The part DE of the waveform is obtained by conduction of T_1, D_1, D_3 & D_4. The part FG of the waveform is obtained by the conduction of thyristors T_1 and T_3 and diodes D_2 and D_4. At $\pi + \alpha$, T_3 is triggered by the waveform K.

(d) Symmetrical pulse width modulation with single pulse per half cycle:

The power circuit is shown in Fig. 5.4(c). The output voltage waveform E_{out} is shown in Fig. 5.5(d). During the

positive half cycle, at the instant B, thyristor T_2 is triggered by the waveform shown in Fig. 5.3(m). At instant E, T_2 is force-commutated by capacitor C_1 (charged in the previous half cycle) by the triggering of thyristor T_2' by waveform 5.3j. During the negative half cycle, at instant F, T_1 is triggered by the waveform of Fig. 5.3(n). At instant I, T_1 is force-commutated by triggering T_1' by the waveform of Fig. 5.3(o).

(e) Asymmetrical triggering:

The power circuit is shown in Fig. 5.4(d). The output voltage waveform is shown in Fig. 5.5(e). During the positive half cycle, at instant A, T_1 is triggered by the waveform of Fig. 5.3(b). At instant C, T_2 is triggered by the waveform shown in Fig. 5.3( ). Thus the waveform ABCDE of Fig. 5.5(e) is obtained.

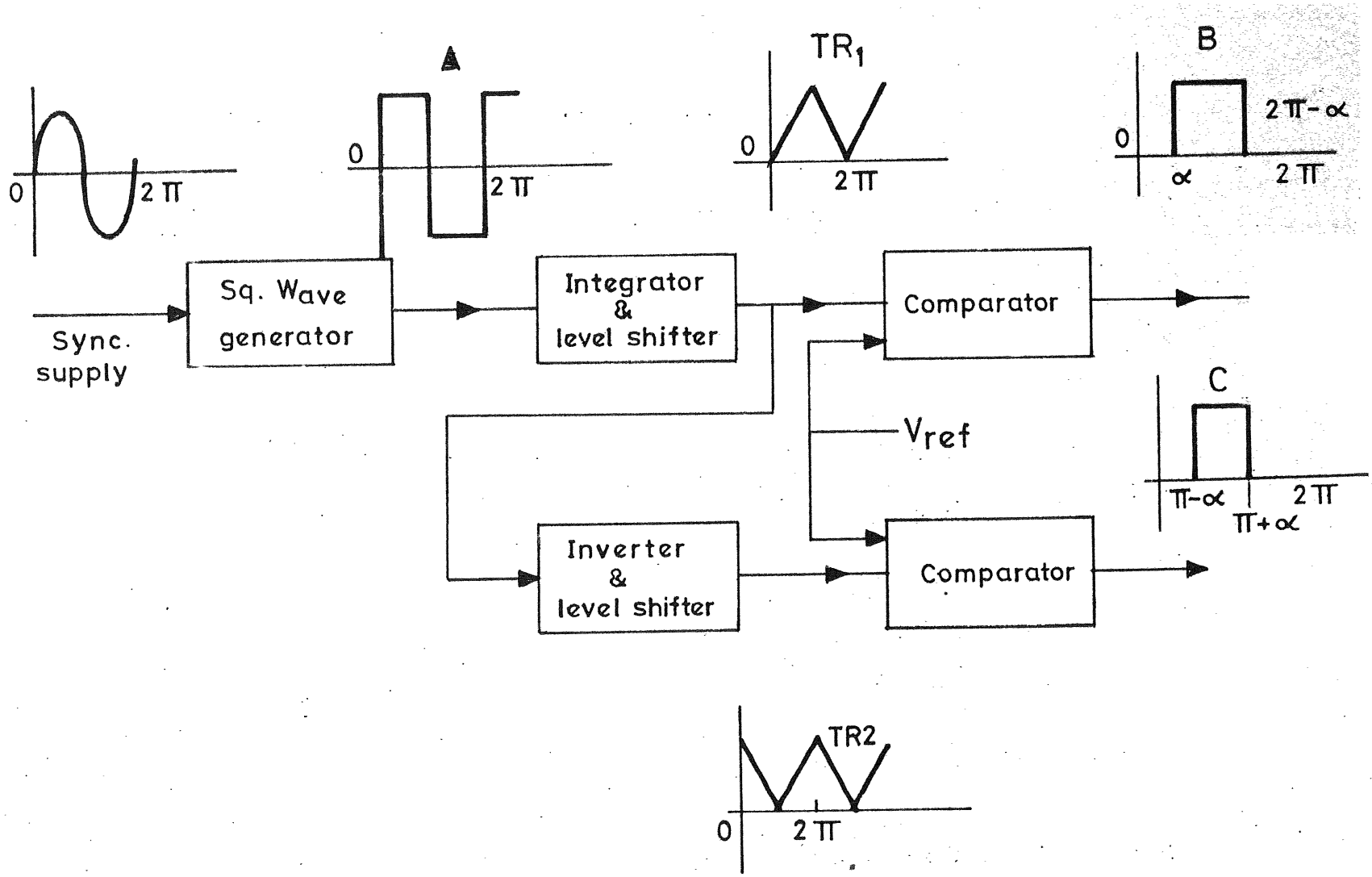
0
2 π
A
0
2 π
TR1
0
2 π
B
0
2 π - α
α
2 π
Sync. supply
Sq. Wave generator
Integrator & level shifter
Comparator
Vref
C
π - α
2 π
π + α
Inverter & level shifter
Comparator
TR2
0
2 π

Fig. 5.1

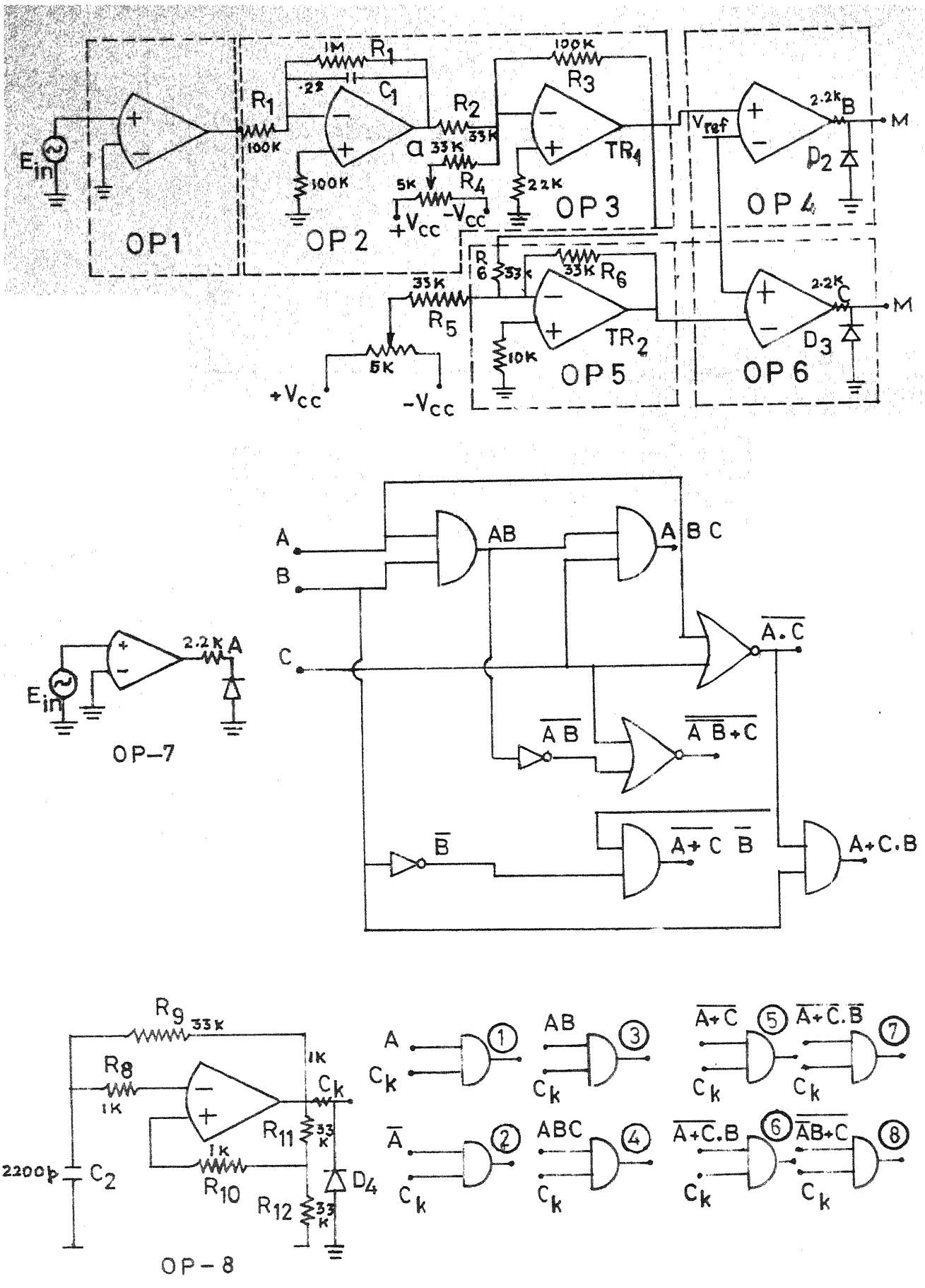

Fig. 5.2 Firing circuit

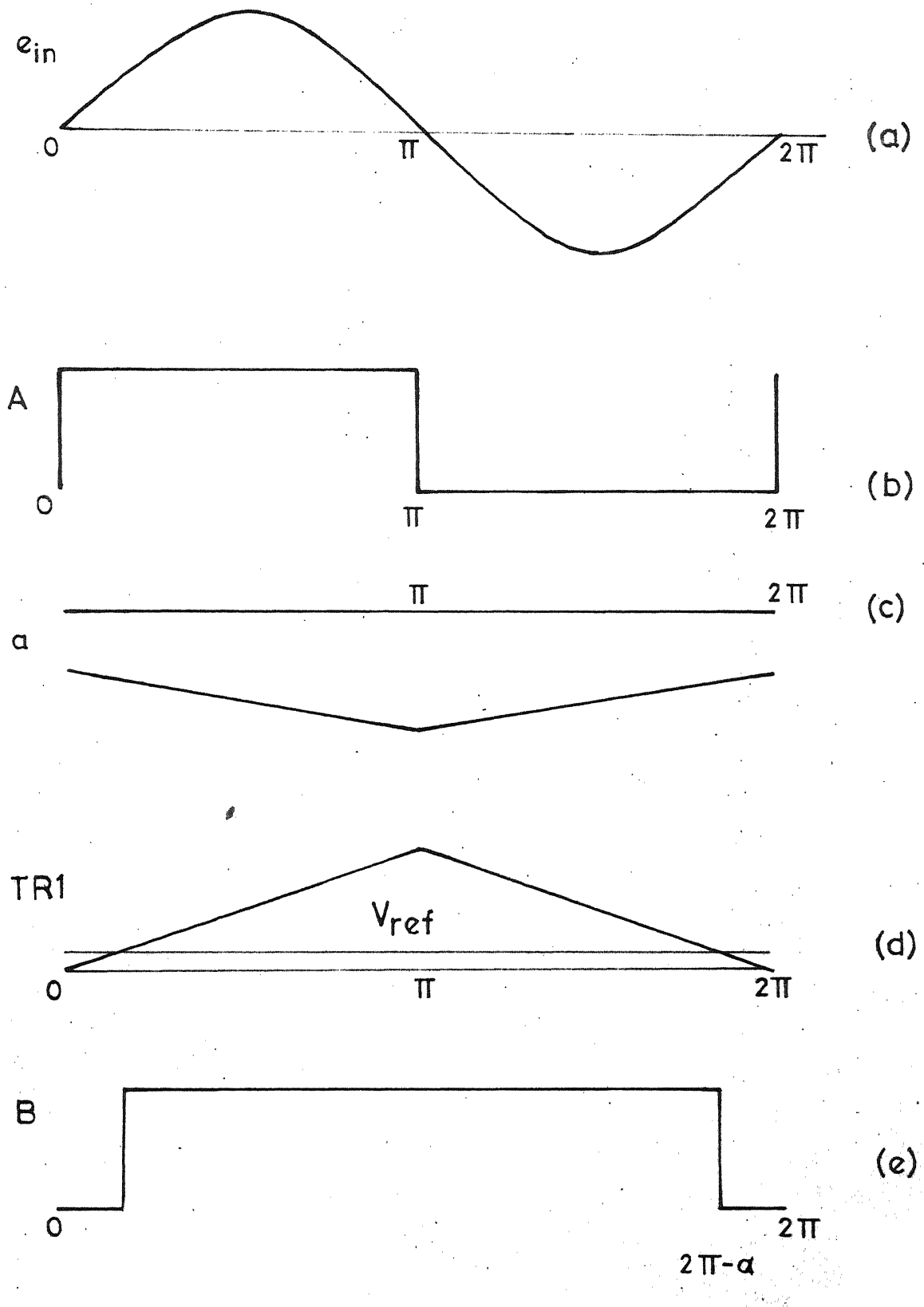

Fig. 5.3 Waveforms at each stage of Fig. 5.2

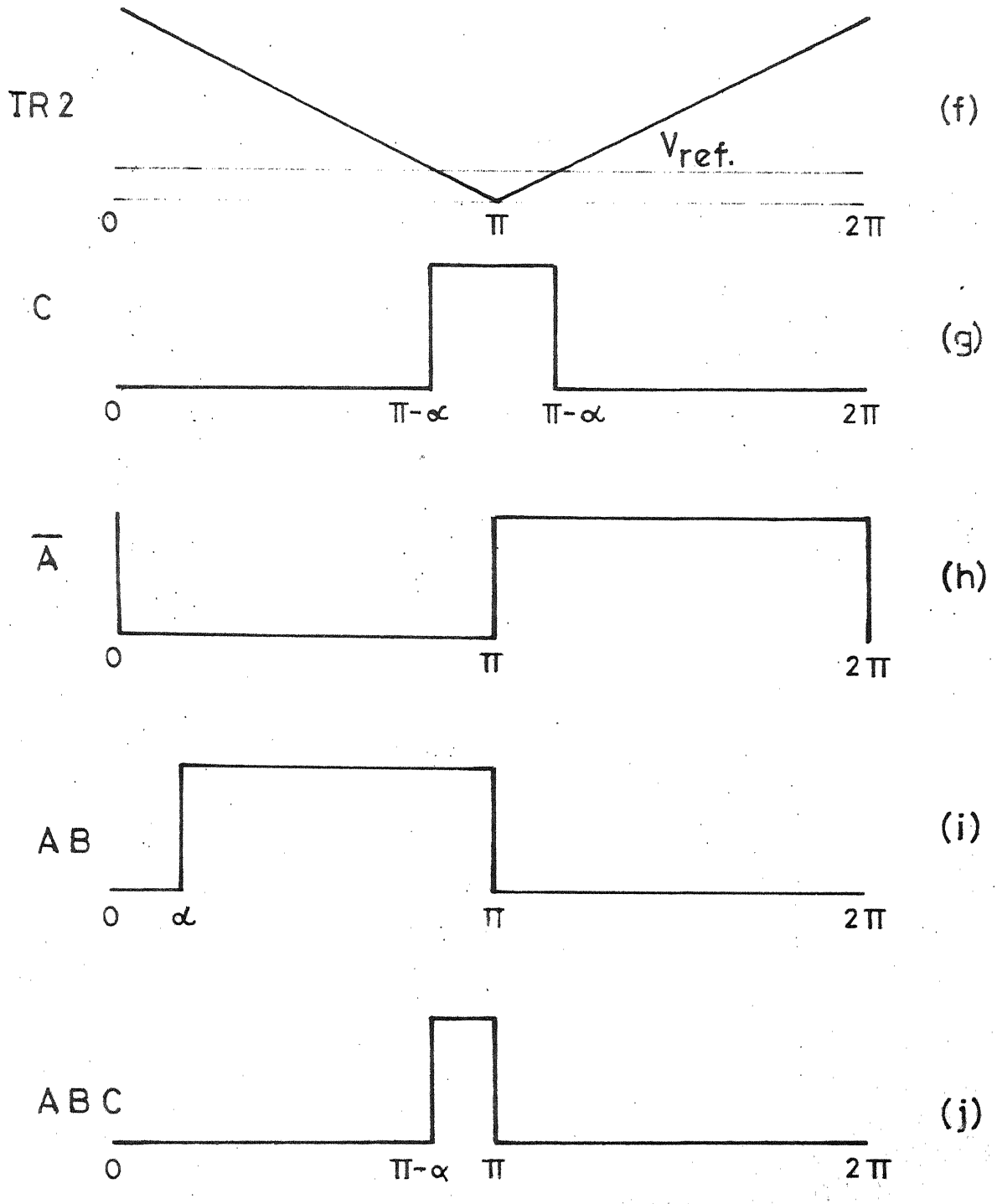
TR 2
(f)
$V_{ref.}$
0
π
2π
C
(g)
0
π-α
π-α
2π
$\overline{A}$
(h)
0
π
2π
A B
(i)
0
α
π
2π
A B C
(j)
0
π-α
π
2π

Fig. 5.3 (Contd.)

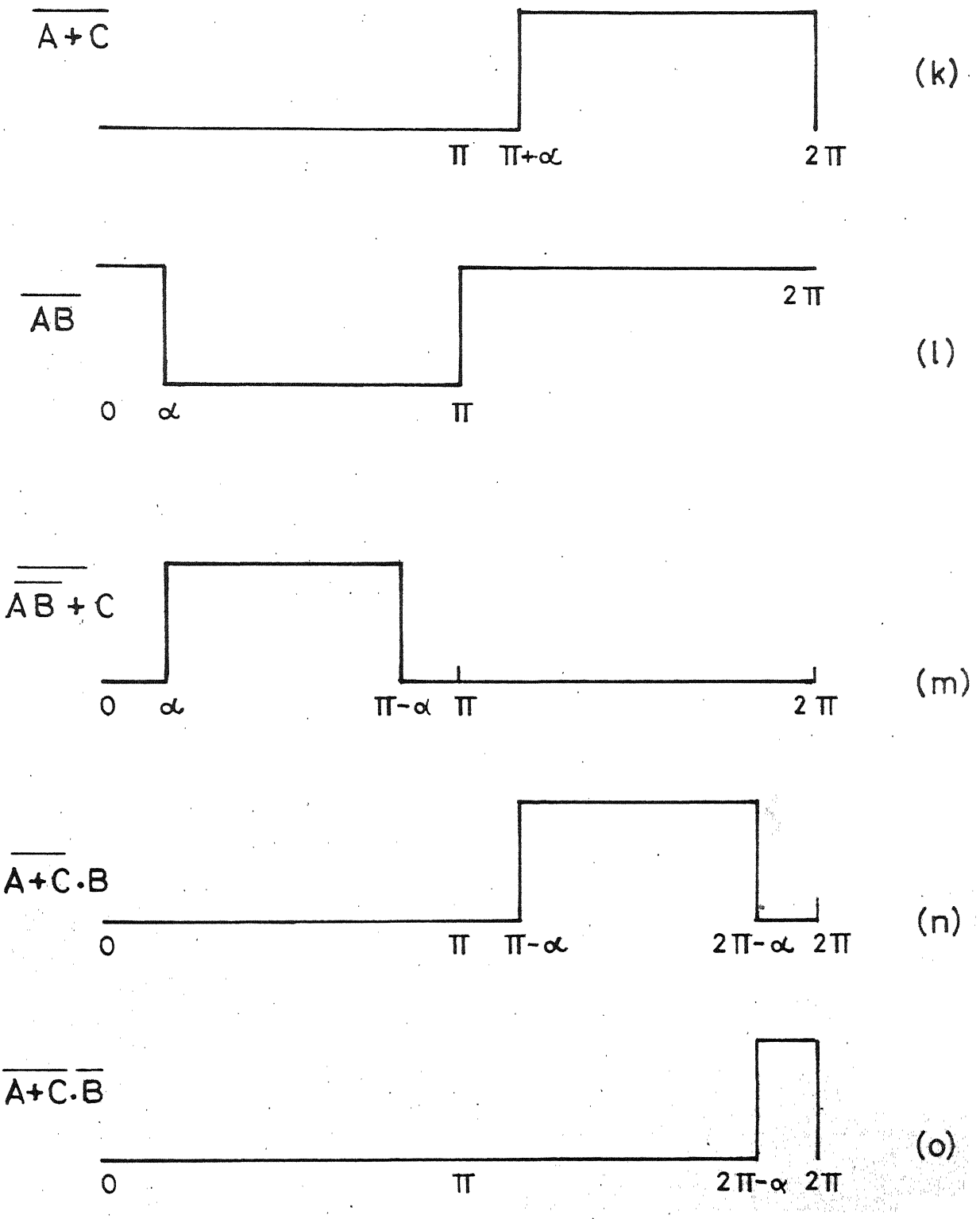
$\overline{A+C}$
(k)
π
π+α
2π
$\overline{AB}$
2π
(l)
0
α
π
$\overline{\overline{AB}+C}$
(m)
0
α
π-α
π
2π
$\overline{A+C}\cdot B$
(n)
0
π
π-α
2π-α
2π
$\overline{A+C}\cdot\overline{B}$
(o)
0
π
2π-α
2π

Fig. 5.3 (contd.)

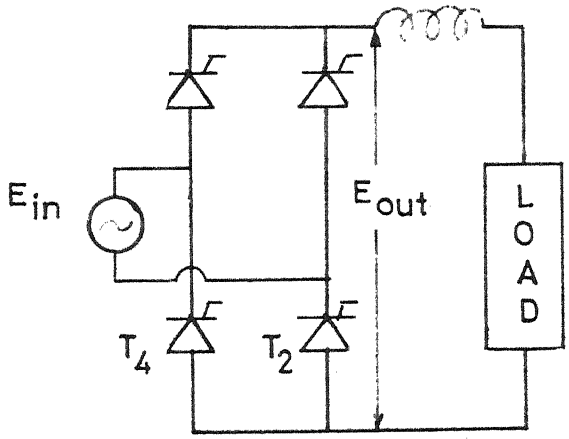

(a)

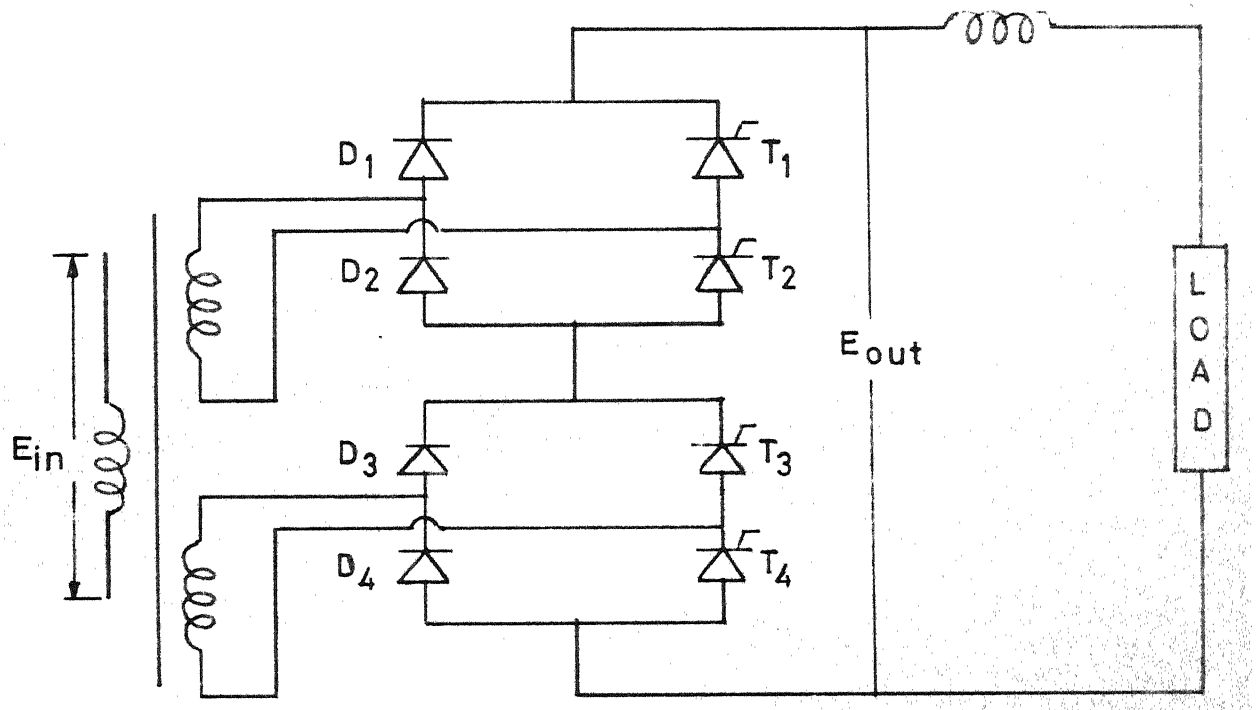

(b)

Fig 5.4 Power circuits

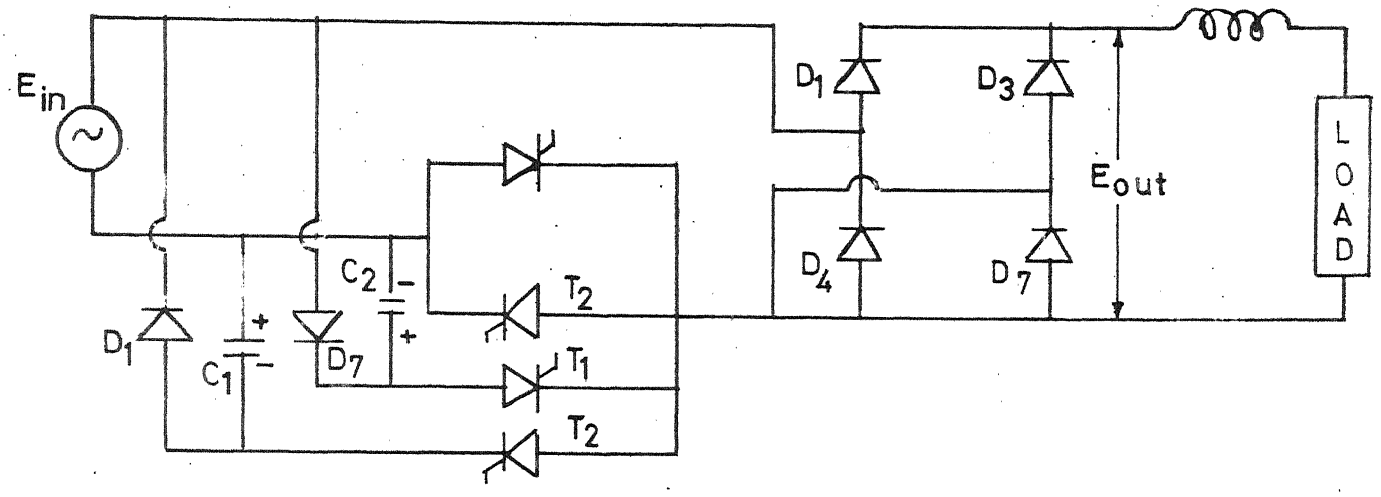

(c)

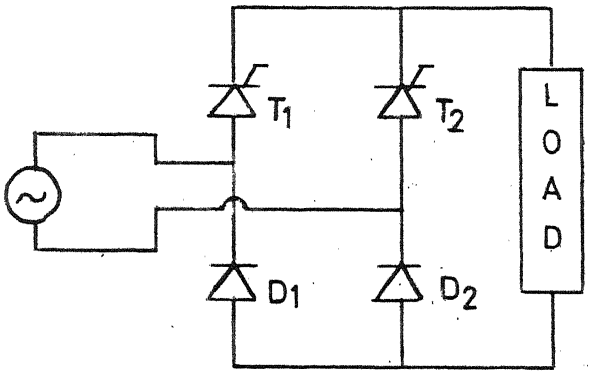

(d)

Fig.5.4 Power circuits (contd.)

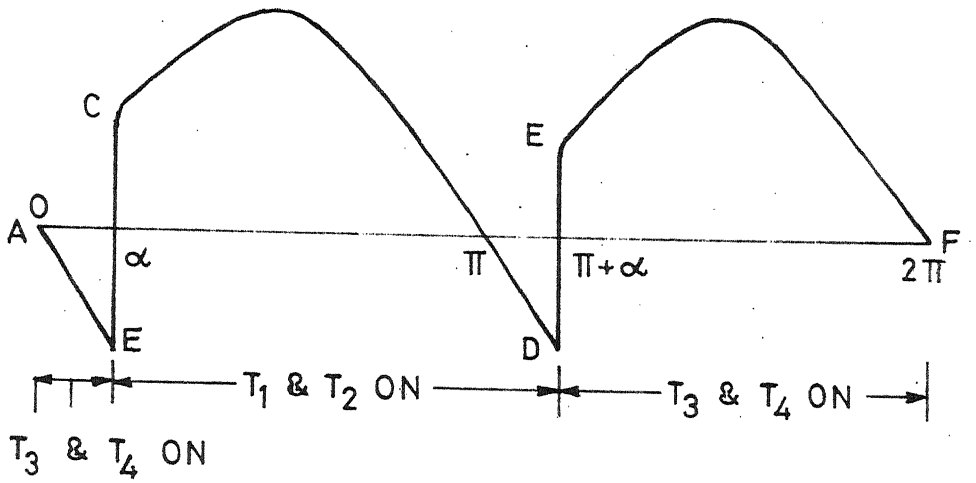

(a)

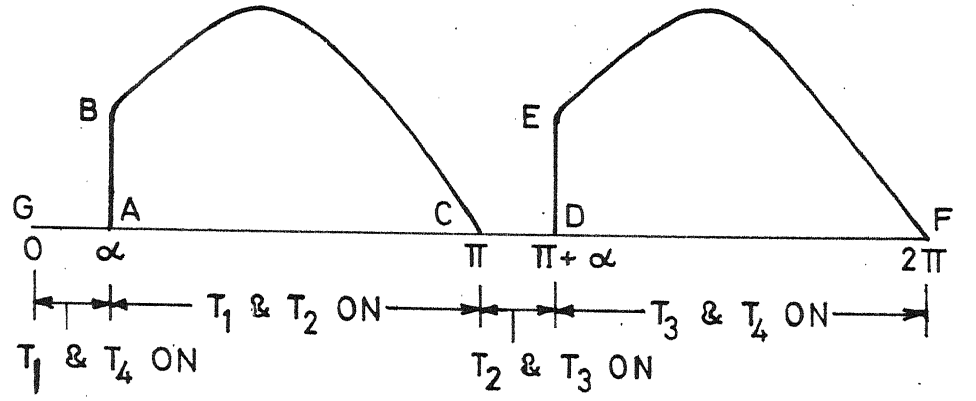

(b)

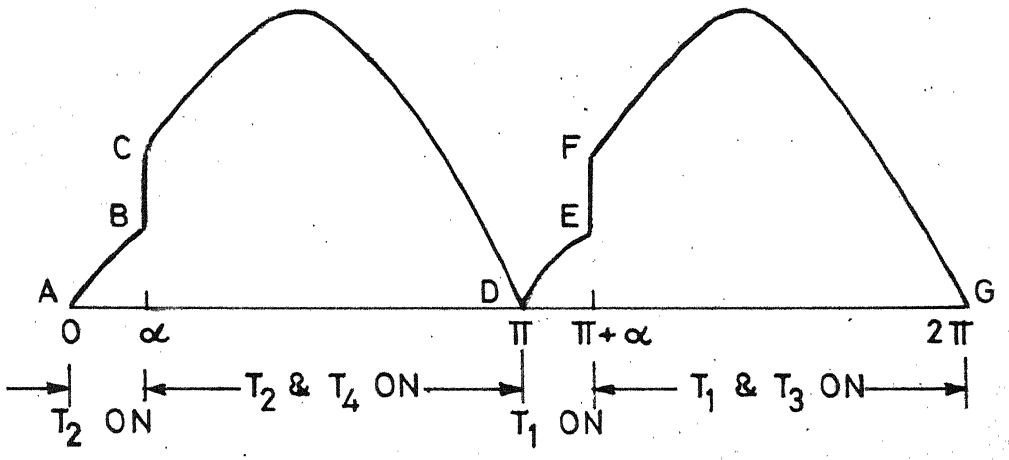

(c)

Fig. 5.5 Output waveforms of Fig. 5.4

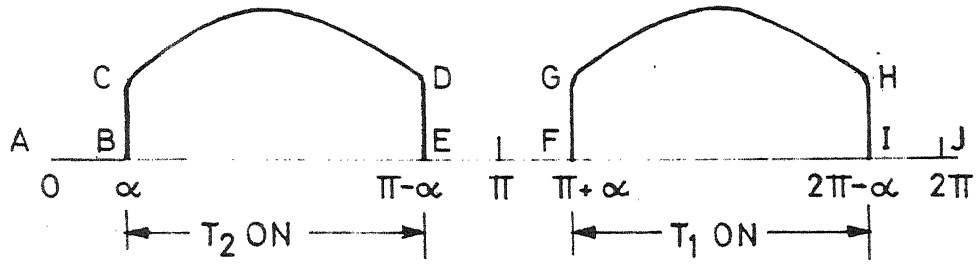

(d)

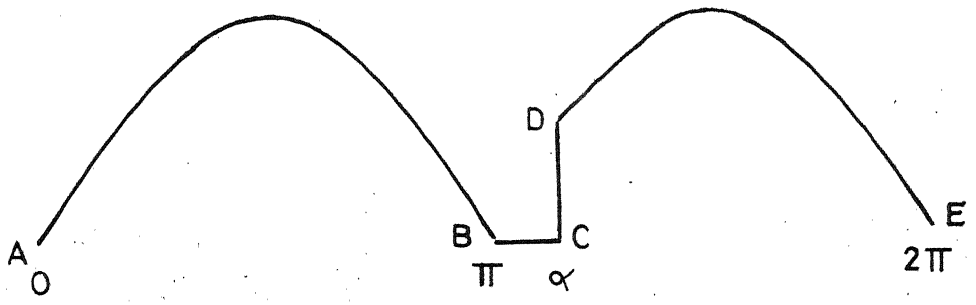

(e)

Fig. 5.5 (contd.)

CONCLUSIONS

From this study the following conclusions can be drawn.

The approach described permits the calculation of motor steady-state performance analytically with less computation time compared to existing methods.

When the d.c. series motor is fed by fully-controlled converter, discontinuous conduction takes place for low values of load torque. The optimum value of inductance which permits elimination of discontinuous conduction and keeps the ripple within acceptable limits can be estimated from monograms given in terms of normalised variables for any d.c. series motor.

For calculating transient response, methods I and II both require much less time as compared with step-by-step method of the two methods, method II is better as it uses second order approximation.

Appendix I

Calculation of Current Ripple

Case I. When motor is fed with fully-controlled converter: continuous conduction, fig.2(a).

The basic equation governing the operation is given by

$$Em \sin wt = R\,i + L\frac{di}{dt} + E \qquad (1)$$

$$\alpha \leq wt \leq \pi + \alpha$$

where $E = (C_o + C_1\, i)\, W_{av}$ using approximation III.

$$L\frac{di}{dt} + Ri + (C_o + C_1\, i)\, W_{av} = Em \sin wt$$

or, $$\frac{d(e^{At} i)}{dt} = \frac{Em}{L} e^{At} \sin wt - \frac{C_o}{L} W_{av} e^{At}$$

where $$A = \frac{R + C_1 W_{av}}{L}$$

Integrating from $\frac{\alpha}{w}$ to t,

$$i(t) = Im(\sin(wt-\phi) - \sin(\alpha-\phi)e^{-A(wt-\alpha)/w}) - \frac{C_o W_{av}}{R+C_1 W_{av}}(1 - e^{-A(wt-\alpha)/w}) + i_1\, e^{-A(wt-\alpha)w} \qquad (2)$$

where $\phi = \tan^{-1}(WL/(R+C_1 W_{av}))$

and $$Im = \frac{Em}{((R+C_1 W_{av})^2 + (WL)^2)^{\frac{1}{2}}}$$

i_1 can be evaluated from the condition

$$i\left(\frac{\pi+\alpha}{w}\right) = i_1$$

i.e., $$i_1 = -Im(\sin(\alpha-\phi) + \sin(\alpha-\phi)e^{-A\pi/w})\,(1-e^{-A\pi/w})^{-1} - C_o W_{av}/(R+C_1 W_{av})$$

Case II: When fed by half-controlled converter, (Fig.2c)

The basic equations are

Duty interval: ($\alpha \leq wt \leq \pi$)

$$Em \sin wt = i R + L \frac{di}{dt} + E \qquad (3)$$

Freewheeling interval: ($0 \leq wt \leq \alpha$)

$$0 = iR + L \frac{di}{dt} + E \qquad (4)$$

where $E = (C_o + C_1 i) W_{av}$ using approximation III

From equation (4),

$$\frac{d}{dt} (e^{At} i) = - \frac{C_o}{L} W_{av} e^{At}$$

Integrating from o to t,

$$e^{At} i - i_1 = + \frac{C_o W_{av}}{AL} (1 - e^{At})$$

or, $$i = i_f = - \frac{C_o W_{av}}{R + C_1 W_{av}} (1 - e^{-At}) + i_1 e^{-At} \qquad (5)$$

From equation (1), multiplying by e^{At},

$$\frac{d}{dt} (e^{At} i) = \frac{Em}{L} \sin wt \, e^{At} - \frac{C_o W_{av}}{L} e^{At}$$

Integrating from α/w to t,

$$i = i_d = \frac{Em}{Z} (\sin(wt - \phi) - \sin(\alpha - \phi) e^{-A(wt-\alpha)/w}) - (C_o W_{av}/(R + C_1 W_{av}))$$

$$(1 - e^{-A(wt-\alpha)/w}) + i_2 e^{-A/w(wt-\alpha)/w} \qquad (6)$$

where $\phi = \tan^{-1} \frac{WL}{R + C_1 W_{av}}$ and $Z = ((R + C_1 W_{av})^2 + (WL)^2)^{\frac{1}{2}}$

From equation (5), $i_2 = i_f(\alpha/w)$

$$\text{i.e., } i_2 = -\frac{C_o W_{av}}{R+C_1 W_{av}}(1-e^{-A\alpha/w}) + i_1 e^{-A\alpha/w} \qquad (7)$$

and from equation (6), $i_1 = i_d\ (\pi/w)$

$$\text{i.e., } i_1 = Im\ (\sin\phi - \sin(\alpha-\phi)e^{-A(\pi-\alpha)/w}) - \frac{C_o W_{av}}{R+C_1 W_{av}}(1-e^{-A(\pi-\alpha)/w}) + i_2\ e^{-A(\pi-\alpha)/w} \qquad (8)$$

where $Im = \frac{Em}{Z}$

Solving equations (7) and (8) simultaneously,

$$i_1 = D\ (1-e^{-A(\pi/w)})^{-1} - C$$

and $i_2 = D\ (-e^{-(A/w)\pi} + 1)^{-1}\ e^{-A\alpha/w} - C.$

where $D = Im(\sin\phi - \sin(\alpha-\phi)e^{-(\alpha-\alpha)A/w})$ & $C = \frac{C_o W_{av}}{R+C_1 W_{av}}$

$$i = i_f = -C + D(1-e^{-A\pi/w})^{-1}\ e^{-At} \qquad (9)$$

for $o \leq wt \leq \alpha$

$$\text{and } i = id = Im(\sin(wt-\phi) - \sin(\alpha-\phi)e^{-A(wt-\alpha)/w}) + D(1-e^{-A\pi/w})^{-1}\ e^{-At} - C \text{ for } \alpha \leq wt \leq \pi \qquad (10)$$

Appendix II

The specifications of the motor used are:

220V, 11.6A, 2.2KW, 1500 RPM, R=2.8Ω, L=0.076H, J=.08 Kg-m^2, B = .01 Nm/rad/sec.

AC supply used: 220V, 50 Hz.

APPENDIX III

+12V 6.3V -12V

0 0 0

Sync Supply

0

Comm Gnd

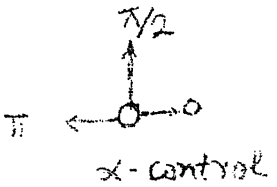

Fully-controlled operation

0 0

T_1, T_2 T_3

0 0

(i) (k)

Fully-controlled/ half-controlled

0 0 0 0

T_1 T_2 T_3 T_4

0 0 0 0

(b) (i) (h) (k)

Asymmetrical Triggering

0 00

T_1 T_2

0 0

(b) (k)

Seq control

0 0 0 0

T_1 T_2 T_3 T_4

0 0 0 0

(h) (b) (k) (i)

Sym PWM

0 0 0 0

T_1 T_2 T_3' T_2'

0 0 0 0

(n) (m) (o) (j)

These are inputs to various pts.

REFERENCES

1. S.R. Doradla and P.C. Sen, 'Solid-state series motor drive', IEEE Trans. IECI, vol. 22, No. 2, pp. 164-71, May,1975.

2. M. Ramamoorthy and B. Ilango, 'The transient response of a thyristor-controlled series motor', IEEE Trans. on PAS, vol. 1, PAS-90, Jan./Feb. 1971, pp. 289-297.

3. S.N. Bhadra, 'Transient response of thyristor-controlled D.C. series motor under small disturbances', Jr. IE(India), vol. 56, Pt. EL4, Feb. 1976.

4. G.K. Dubey, 'Calculation of filter inductance for chopper fed d.c. separately-excited motor', Proc. IEEE, vol. 66, No. 12, 1978, pp. 1671-73.

5. F.E. Edwin and G.K. Dubey, 'Transient analysis of converter-controlled d.c. separately excited motor', Jr. of Electric Machines and Electromechanics, vol. 2, No. 4, pp. 325-402, 1978.

6. G.K. Dubey and W. Shepherd, 'Transient analysis of chopper-controlled d.c. series motor', IEEE Trans. IECI, vol. 28, No. 2, pp. 146-59, May,1981.

7. G.K. Dubey and W. Shepherd, 'Analysis of d.c. series motor fed by power pulses', Proc. IEE, vol. 122, pp. 1397-78, Dec. 1975.

8. V. Subbaiah and S. Palanichamy, 'Mode identification and minimum inductance estimation for fully-controlled thyristor converters', IEEE Trans. IECI, vol. 26, Feb. 1979, pp. 48-50.

9. P. Mehta and S. Mukhopadhyay, 'Modes ofoperation of converter-controlled d.c. drives', Proc. IEEE, vol. 121, No. 3, pp. 179-183, March,1974.

10. P.B. Anjaneyulu , 'Studies on converter-fed d.c. drives', M.Tech. thesis, I.I.T. Kanpur, 1979.

11. J. Millman and C.C. Halkias, 'Integrated Electronics: Analog and Digital Circuits and Systems', Kogakusha, McGraw-Hill, 1972.